International Journal of Biological Macromolecules 231 (2023) 123339

Contents lists available at ScienceDirect

International Journal of Biological Macromolecules

journal homepage: www.elsevier.com/locate/ijbiomac

In vitro evaluation of alkaline lignins as antiparasitic agents and their use as an excipient in the release of benznidazole

Iranildo José da Cruz Filho [a,*], Denise Maria Figueiredo Araujo Duarte [b], Douglas da Conceição Alves de Lima [a], Diego Santa Clara Marques [a], Fábio André Brayner dos Santos [c], Luiz Carlos Alves [c], André de Lima Aires [d], Fátima Nogueira [b], Maria do Carmo Alves de Lima [a]

[a] Federal University of Pernambuco, Department of Antibiotics, Biosciences Center, 50, 670-420 Recife, PE, Brazil
[b] Global Health and Tropical Medicine, GHTM, Institute of Hygiene and Tropical Medicine, IHMT, Universidade Nova de Lisboa, 1349-008 Lisbon, Portugal
[c] Aggeu Magalhães Institute, Oswaldo Cruz Foundation (IAM-FIOCRUZ), 50670-420 Recife, PE, Brazil
[d] Laboratory of Immunopathology and Infectious-Parasitic Diseases Keizo Asami – LIKA, 50670-420 Recife, PE, Brazil

ARTICLE INFO

Keywords:
Lignins
Antioxidants
Antiparasitic

ABSTRACT

The Amazon rainforest is considered the largest tropical timber reserve in the world. The management of native forests in the Amazon is one of the most sensitive geopolitical issues today, given its national and international dimension. In this work, we obtained and characterized physicochemical lignins extracted from branches and leaves of *Protium puncticulatum* and *Scleronema micranthum*. In addition, we evaluated *in vitro* its potential as an antioxidant, cytotoxic agent against animal cells and antiparasitic against promastigotes of *Leishmania amazonensis*, trypomastigotes of *T. cruzi* and against *Plasmodium falciparum* parasites sensitive and resistant to chloroquine. The results showed that the lignins obtained are of the GSH type and have higher levels of guaiacyl units. However, they show structural differences as shown by spectroscopic analysis and radar charts. As for biological activities, they showed antioxidant potential and low cytotoxicity against animal cells. Anti-leishmanial/trypanocidal assays have shown that lignins can inhibit the growth of promastigotes and trypomastigotes *in vitro*. The lignins in this study showed low anti-*Plasmodium falciparum* activity against susceptible strains of *Plasmodium falciparum* and were able to inhibit the growth of the chloroquine-resistant strain. And were not able to inhibit the growth of *Schistosoma mansoni* parasites. Finally, lignins proved to be promising excipients in the release of benznidazole. These findings show the potential of these lignins not yet studied to promote different biological activities.

1. Introduction

Lignins are amorphous three -dimensional macromolecules with complex and variable molecular structure, which depends on plant species, location, plant age, climate station, extraction and obtaining methods among others [1,2]. Although its chemical structure has not yet been fully elucidated, mainly due to the changes it undergoes during the extraction and obtaining process [3]. It is known that lignins can be defined as a class of natural polyphenolic macromolecules [3,4]. These originate from a dehydrogenative polymerization, catalyzed by free radical enzymes, of the cinnamyl acid precursors of three phenyl-propanoid monomers, the coniferyl, sinapyl and *p*-coumarin alcohols [1,2,4]. When these are incorporated, the lignins are called guaiacyl (G), syringyl (S) and *p*-hydroxyphenyl (H), which are joined by C—O—C and C—C bonds, in addition to having different functional groups (aliphatic and aromatic hydroxyls, ethers, carbonyls and methoxyls) [1–4].

Industrially, lignins are obtained as a co-product of the kraft pulping process (a process used by the pulp and paper industries) which produces cellulosic pulp and a black liquor rich in lignins [4]. On average, around 40 to 50 million tons of black liquor (lignin) are generated each year [3]. These data show that lignins are a renewable and abundant resource [3,4]. Lignins have great versatility of applications, they can be used for the production of energy, fuels, chemical products, building materials and supercapacitor electrodes [1,2,5]. In addition to promoting different biological activities, which increase the added value and interest in studies focused on the biomedical and pharmaceutical areas [6].

Biological activities are related to the structure of lignins, that is, the

* Corresponding author.
E-mail address: iranildoj@gmail.com (I.J. da Cruz Filho).

https://doi.org/10.1016/j.ijbiomac.2023.123339
Received 12 December 2022; Received in revised form 10 January 2023; Accepted 15 January 2023
Available online 20 January 2023

wide variety of functional groups (phenolic and aliphatic hydroxyl, methoxyl, carbonyl, carboxyl and quinone, among others) and chemical bonds, which together can promote different activities [6–7]. The literature reports different activities promoted by lignins, among which we can mention: antioxidant activity [8,9], immunomodulatory [10], cytotoxic [8,9], antimicrobial [11], antileishmania [12], anti-*Plasmodium falciparum* (agent etiologic agent of malaria) [13], anticancer, antiviral, among others [6]. Furthermore, they can be used as materials for the production of hydrogels as fast-release drug carriers for ribavirin [14]. They can also be used as a material for the release of drugs [15]. Therefore, the search for new lignins or their functionalization can enhance activities [6,7].

The Amazon Forest has a great diversity of plant species, which can be studied to obtain different lignins [13,16]. Among the Amazonian species we can mention: *Protium puncticulatum* and *Scleronema micranthum* trees used in a sustainable way by the timber sector [17,18].

In this study we evaluated the lignins of branches and leaves of *Protium puncculatum* and *Scleronema micranthum*. These regions (branches and leaves) were chosen because they are easily obtained during pruning without causing major damage to these trees [10]. These lignins not yet studied were obtained by acid pre-treatment followed by alkaline delignification. Then they were characterized by different spectroscopy techniques to assess their chemical structure. Finally, the antioxidant, cytotoxic and antiparasitic potential was evaluated in animal cells against the promastigotes strains *Leishmania amazonensis*, *Trypanosoma cruzi*, *Plasmodium falciparum* 3D7 sensitive to chloroquine and *Plasmodium falciparum* (Dd2) resistant to chloroquine. And before the young and adult worms of *Schistosoma mansoni*. In addition, the evaluated lignins proved to be efficient excipients in formulations for the release of benznidazole. This study contributes to the use of lignins as antiparasitic agents.

2. Materials and methods

2.1. Material plant

The branches and leaves of the species *Protium puncticulatum* and *Scleronema micranthum* were provided by the company Mil Madeiras Preciosas Ltda (PRECIOUS WOODS) located in the municipality of Itacoatiara in the State of Amazonas, Brazil. The species were registered in SisGen (National System of Genetic Heritage and Associated Traditional Knowledge), n° ACE6CCF and A36E658 respectively. The branches and leaves were dried at 60 °C for 48 h in an oven (Tecnal, TE-393/1), then they were ground in a knife mill (Fritsch – Pulverisette 14) and sieved in a granulation of 80 mesh. Finally, they were stored at 30 °C.

2.2. Analysis of chemical composition from branches and leaves of Protium puncticulatum and Scleronema micranthum species

The branches and leaves from *Protium puncticulatum* and *Scleronema micranthum* species were characterized according to the procedure described by Silva et al. [12] and Araujo et al. [13] obtaining the chemical composition regarding the contents of cellulose, hemicellulose, lignin, extractives and ash. Initially, the moisture content was determined, 20 g of branches or leaves were dried at 105 ± 2 °C in an oven (Tecnal, TE-393/1) until constant weight (72 h). The moisture content was determined gravimetrically. The dried material was subjected to extraction in a Soxhlet apparatus using a toluene:ethanol (38:62 v/v) extraction system for 8 h, the final mass was dried (105 ± 2 °C for 72 h) and the extractives content also obtained by gravimetry.

The determination of polysaccharides was performed by acid hydrolysis (2 g of plant biomass, free of extractives, 12 mL of 72 % H_2SO_4, 45 °C, 7 min). The cellulose and hemicellulose contents depend on the carbohydrate and organic acid concentrations present in the hydrolyzate. After hydrolysis, the reaction mixture is filtered through previously dried and tared filter paper. The concentrations of carbohydrates and organic acids were determined by high performance liquid chromatography (HPLC), under the following conditions: Aminex HPX87H column (Bio-Rad), temperature of 60 °C, mobile phase: H_2SO_4 5 mM, flow rate of 0.6 mL/min and detector (RI) refractive index for the identification and quantification of the components (cellobiose, glucose, xylose, arabinose, formic acid, acetic acid). The concentration of furfural and HMF was determined using a reversed phase column (C-18) (Agilent Technologies), with a mobile phase composed of a solution of acetonitrile-water-acetic acid 1:8:1 %, using a UV/Vis detector (274 nm) at 25 °C. The samples were filtered through a 0.22 μm membrane before the analytical procedure.

The solid material retained on the filter paper corresponds to insoluble lignin. The total ash content is the residue after the ignition of 2 g of biomass at 800 °C for 2 h. The lignin content was determined by subtracting the cellulose, hemicellulose, extractives, moisture and ash contents from 100 % of the biomass sample.

2.3. Obtaining lignins from branches and leaves of Protium puncticulatum and Scleronema micranthum species

Lignins were obtained according to the methodology described by Cruz-Filho et al. [8], Santos et al. [9], Melo et al. [11], Silva et al. [12] and Araújo et al. [13] with few modifications in a four-step process. Initially (Step I), the crushed material (1.0 kg) was subjected to extraction using a cyclohexane/ethanol extractor system (50:50, v/v) in a 5 L glass flask (hermetically closed) under maceration for one week (solid: liquid ratio 1:4 w/v). At the end of the extraction, the material was filtered. The solid fraction was dried to constant weight at 105 ± 2 °C in an oven for 72 h.

The dry solid (Stage II) was subjected to a treatment with diluted acid using 2 % H_2SO_4 in solid: liquid ratio (1:5 w/v) the system was subjected to 120 °C for 1 h in a Regmed AU model reactor/E-20. The system was filtered and the solid dried to constant weight. These two steps were performed to remove polar and non-polar molecules and polyoses. Then, the dry solid was subjected to an alkaline delignification with 1 % NaOH under the same conditions of acid hydrolysis (Step III). Aiming at the removal of lignins (liquid fraction) and cellulose (solid fraction).

At the end of the process, the solid was separated from the black liquor by filtration and the black liquor was acidified with H_2SO_4 to pH 2 to precipitate the lignin and the mixture was incubated at 30 °C for 12 h without stirring (Step IV). At the end of this period, the lignin was filtered and washed carefully until neutrality and then dried at 70 ± 2 °C for 24 h. The yield of obtaining lignin was obtained by Eq. (1).

$$Y\ (\%) = \left(\frac{\text{Mass of lignin extracted}}{\text{Total lignin mass total mass in branches or leaves}}\right) * 100\% \quad (1)$$

2.4. Physicochemical characterization of lignins from branches and leaves of Protium puncticulatum, and Scleronema micranthum species

2.4.1. Elementary analysis

A sample of 2 mg of lignin was dried in an oven at 105 ± 2 °C and, later, placed in a Vario Micro Cube elemental analyzer, obtaining the contents of nitrogen, carbon, hydrogen, sulfur and, by difference, the content of oxygen. The combustion and reduction tube temperatures were 1200 °C and 850 °C, respectively, using helium as carrier gas and oxygen as oxidizing gas.

2.4.2. Fourier transform infrared spectroscopy (FTIR)

Lignins (20 mg) were analyzed using a Shimadzu IR Tracer-100 spectrometer. The spectra were obtained in the wavelength range from 400 to 4000 cm^{-1} for the identification of functional groups present in the structures. The experiments were carried out in triplicate according to the methodology proposed by Santos et al. [9], Melo et al. [11], Silva et al. [12] and Araújo et al. [13].

2.4.3. Spectroscopic analysis in the ultraviolet/visible (UV–Vis) region

UV/Vis spectroscopic analyzes are performed in order to obtain information on the aromatic structure of lignins. These experiments were carried out according to the methodology proposed by Melo et al. [11], Silva et al. [12] and Araújo et al. [13] with few modifications. Initially, the lignins were solubilized in a 0.01 mol/L sodium hydroxide solution at a concentration of 0.05 g/L. Spectra were obtained in the range of 190 to 400 nm in a spectrophotometer (Hewlett-Packard, model 8453). This experiment was carried out in order to obtain the maximum absorption wavelength. Then, the lignin solutions at a concentration of 0.05 g/L were diluted in concentrations ranging up to 0.001 g/L to determine the extinction coefficient (absorptivity), an important parameter to determine how much the lignin structure is condensed. All experiments were performed in triplicate.

2.4.4. Acetylation of lignin and characterization by nuclear magnetic resonance (HSQC NMR)

In order to increase the solubility of lignin in organic solvents, an acetylation reaction was carried out on the sample. Acetylation was performed according to the procedure described by Cruz-Filho et al. [8], Santos et al. [9], Melo et al. [11], Silva et al. [12] and Araújo et al. [13] with few modifications. For this, 100 mg of lignin was subjected to a 1:1 pyridine-acetic anhydride solution in a N_2 atmosphere for 30 min. After this period, the system was allowed to react for 100 h. After acetylation, the lignin was purified with extensive washes with ethyl ether. After this process, the lignin was dried in a lyophilizer. After drying, 10 mg was solubilized in deuterated DMSO (DMSOd6) and analyzed in a BRUKER Avance 400 MHz spectrometer.

2.4.5. Determination of the molecular weight of lignins by Gel Permeation Chromatography (GPC)

Assays to determine the molecular weight of lignins were performed according to Santos et al. [9], Melo et al. [11], Silva et al. [12] and Araújo et al. [13]. Initially, the lignins were dissolved in 0.5 M NaOH at a concentration of 4 mg/mL. The chromatography system consisted of a glass column (57 cm × 1.8 cm) packed with Sephadex G-50 equilibrated in 0.5 M NaOH. The column was loaded with sample and eluted with 0.5 M NaOH at a flow rate of 0.4 mL/min. Fractions of 4 mL were collected and the absorbance was determined at 280 nm with a Hewlett-Packard® spectrophotometer against a blank of NaOH solution. The column was calibrated with previously determined mass standards.

Through the results obtained, it was possible to determine the numerical average molecular weight (Mn), weight average molecular weight (Mw) and Mw/Mn ratio (dispersibility).

2.4.6. Thermogravimetric analysis (TGA) and differential thermal analysis (DSC)

Analyzes were performed using a simultaneous thermal analyzer (STA 6000, PerkinElmer). Samples with about 10 mg lignin. Each sample was analyzed in the temperature range of 30 to 650 °C, with a heating rate of 10 °C/min. The experiments were carried out in triplicate according to the methodology proposed by Silva et al. [12] and Araújo et al. [13].

2.4.7. Analytical fast pyrolysis (PY-GC/MS)

The lignin pyrolysis assays were performed by Silva et al. [12] and Araujo et al. [13] with slight adaptations. Assays were performed using a fast pyrolysis analyzer coupled to GC/MS (Agilent Technologies 7890A /5975C) in order to investigate the distribution of volatiles from fast pyrolysis of lignin. Therefore, 10 mg samples were added to the pyrolysis tube and the temperature was adjusted to 550 °C, the instantaneous heating rate was 20,000 °C/s and the residence time was 45 s. The volatile constituents were identified by GC/MS (model QP2010, Shimadzu), with a DB-35MS capillary column (5 m × 0.20 mm × 0.33 μm CGMS Agilent) under the conditions: helium gas with a flow of 1 mL/min, inlet temperature 300 °C, the oven temperature was programmed from 40 °C (3 min) to 200 °C (1 min) with a heating rate of 4 °C/min and then to 280 °C (1 min) with a heating rate of 20 °C/min; mass spectra were operated in electron ionization (EI) mode at 70 eV. Mass spectra were obtained from *m/z* 50 to 650.

2.4.8. Determination of the content of phenolic groups present in the chemical structure of lignins

The determination of the total phenolic content present in the lignin structures of this study was performed by means of spectroscopy in the visible region using the Folin-Ciocalteau method, following the methodology described by Cruz-Filho et al. [8], Santos et al. [9], Melo et al. [11], Silva et al. [12] and Araújo et al. [13] with modifications. The lignins were dissolved in a 10 % DMSO solution at a concentration of 1000 μg/mL. Initially, 1 mL of lignin, 1 mL of Folin-Ciocalteau (1:10 v/v), 2 mL of sodium carbonate (20 %), 2 mL of distilled water were added and homogenized. The readings, in a spectrophotometer at 700 nm, were performed at 30 min. The reading blank was 1 mL of distilled water, adding all the reagents mentioned above. The total phenolic content was determined by interpolation of the absorbances of the samples in an analytical curve constructed with standard solutions of gallic acid (3.9-2000 μg/mL) and expressed in mg of EAG (gallic acid equivalents) per g of lignin. All analyzes were performed in triplicate and in the dark.

2.5. Evaluation of in vitro antioxidant activity promoted by lignins

The evaluation of the antioxidant activity was determined following the methodology described by Cruz-Filho et al. [8], Santos et al. [9], Melo et al. [11], Silva et al. [12] and Araujo et al. [13] with some adaptations. The lignins were dissolved in a 10 % DMSO solution at concentrations ranging from 3.9 to 1000 μg/mL. The tests carried out were DPPH, ABTS, phosphomolybdenum and reduction of iron ions.

DPPH radical scavenging assays were carried out in the absence of light, 0.1 mL of each sample concentration was transferred to test tubes containing 3.9 mL of 0.06 mM DPPH methanolic solution and the solutions were homogenized in a water shaker. Tubes. The negative control consisted of 0.1 mL of methanol with 3.9 mL of DPPH solution. Assays were incubated for 30 min. At the end of the reactions, readings were taken in a Hewlett-Packard® spectrophotometer at a wavelength of 515 nm, using methanol as a "blank".

For the ABTS radical scavenging method, the ABTS• + cation was prepared by 5 mL of ABTS• + stock solution with 88 μL of potassium persulfate solution. The mixture was allowed to stand in the dark for 16 h at room temperature. The ABTS• + solution was diluted in methanol until an absorbance of 0.7 ± 0.02 was obtained at 734 nm. In a dark environment, 140 μL aliquots (3.9 to 1000 μg/mL) of lignins were transferred to 2 mL Eppendorf tubes with 1860 μL of ABTS• + radical solution and incubated for 20 min. After this period, the absorbances were recorded. The blank consisted of all reagents and distilled water.

Total antioxidant capacity was assessed by phosphomolybdenum assay. A 0.1 mL aliquot of lignin solution (3.9 to 1000 μg/mL) was combined with 1 mL of reagent solution (600 mM sulfuric acid, 28 mM sodium phosphate and 4 mm ammonium molybdate). The tubes were incubated in a boiling water bath at 90 °C for 90 min. Afterwards, the absorbance was measured at 695 nm against a blank (1 mL of reagent and 0.1 mL of water).

For the iron reduction method, 0.25 mL of phosphate buffer, 0.25 mL of potassium ferrocyanide and 0.1 mL of lignin were initially added at different concentrations and incubated at 50 °C. After 20 min, 0.25 mL of trichloroacetic solution was added and centrifuged at 650 ×*g* for 10 min. 0.5 mL of supernatant was collected, which was mixed with 0.5 mL of distilled water and 0.1 mL of iron chloride. Absorbances were read spectrophotometrically at 700 nm. The blank was constituted with all the reagents and distilled water.

All experiments were performed in triplicate and the standards used were ascorbic acid and butylated hydroxytoluene (BHT) under the

respective test conditions. The concentration at 50 % (IC_{50}) was calculated from a linear curve, obtained graphically by plotting the concentration of the samples in relation to the corresponding effect of inhibition of the antioxidant activity.

2.6. Cytotoxicity assays against mammalian cells

Cell viability was determined by the MTT method (3-methyl-[4–5-dimethylthiazol-2-yl]-2,5-diphenyltetrazolium bromide), as described by Silva et al. [12] and Araújo et al. [13] with few modifications. Macrophages of the J774.A1 lineage, Chinese hamster lung fibroblasts (V79), Vero and Hepg2 (hepatoma) cells were seeded separately (1×10^5 cells/well) in 96-well plates containing RPMI medium with phenol red supplemented with phenol red and incubated in an atmosphere of 5 % CO_2 at 37 °C. After 24 h of cultivation, different concentrations (6.25–100 μg/mL) of lignins diluted in 0.01 % DMSO were added. The lignin system and cells were kept in an oven at 37 °C and 5 % CO_2 for 72 h.

After 72 h of incubation, 20 μL of MTT solution (5 mg/mL) were added. After 4 h of incubation at 37 °C in an oven with a humid atmosphere containing 5 % CO_2, the supernatant was removed and the formed formazan crystals were dissolved in 100 μL of DMSO. then the system was analyzed in a Benchmark Plus ELISA plate reader (Bio-Rad, California, USA) at a wavelength of 540 nm. The experimental control consisted only of cells grown in culture medium. The experiments were performed in triplicate and biological replication. Cell viability was calculated using Eq. (2).

$$\text{Cellular viability}(\%) = \left[\frac{(\text{ABS sample} - \text{ABS blank})}{\text{ABS negative control} - \text{ABS blank}}\right] \times 100 \quad (2)$$

where: ABS sample is the amount of viable cells at different lignin concentrations, ABS negative control is the concentration of viable cells in the control (only cells and culture medium) which represents 100 % viability, ABS of the experiment blank.

The value of CC_{50} (Concentration capable of inhibiting cell growth by 50 %) was obtained by calculating the non-linear regression of the curves obtained in the graphs of Percentage of viability *versus* molar concentration of the lignins under study. The graphs were built using the GraphPad Prism program, version 5.0 for Windows. In addition to lignins, the following drugs were used: amphotericin B, benznidazole, praziquantel, chloroquine and dihydroartemisinin respectively.

2.6.1. In vitro hemolytic activity

The hemolytic test, used to assess *in vitro* toxicity, was performed according to Araujo et al. [13] with few modifications. Initially, erythrocytes from mouse blood were diluted in saline phosphate buffer. Erythrocytes were plated in 96-well plates that received different concentrations (6.25–100 μg/mL) of lignins dissolved in 1 % DMSO. After 1 h, the supernatant was separated by centrifugation at 3000 rpm for 10 min and pipetted into a 96-well plate. Optical density was measured at a wavelength of 543 nm in order to verify hemoglobin release (hemolysis). Phosphate buffered saline was the 0 % hemolysis control and Triton X-100 was the 100 % control. All experiments were performed in triplicate. in addition to lignins, the following drugs were used: amphotericin B, benznidazole, praziquantel, chloroquine and dihydroartemisinin respectively. This study was approved by the Ethics Committee for the Use of Animals of the Aggeu Magalhães Institute/Oswaldo Cruz Foundation, protocol number 164/2020.

2.7. In vitro leishmanicidal activity

2.7.1. Cultivation and growth kinetics of the promastigote forms of *Leishmania amazonensis*

Promastigote forms of *Leishmania amazonensis* (strain WHOM/00LTB0016) were maintained at 26 °C in supplemented Schneider medium (20 % fetal bovine serum and 1 % penicillin-streptomycin solution), pH 7.2. Parasites in the exponential phase of growth were used in all experiments with re-raising every three days. The promastigote forms were submitted to three washing cycles with ice-cold sterile saline, with centrifugation at 3000 rpm, for 15 min at 4 °C and adjusted with Schneider medium to the desired concentrations in each experiment. The viability of the parasites was analyzed by their motility under an optical microscope.

The growth kinetics of the parasites was performed according to Silva et al. [12] in 96-well plates the parasites were incubated in an atmosphere of 5 % CO_2 at 37 °C and for a period ranging from 0 to 96 h the growth was monitored by counting in a Neubauer chamber. Growth velocity and generation time were determined by Eqs. (3) and (4) respectively.

$$ln\frac{X}{X_0} = \mu max.t \quad (3)$$

$$t_g = \frac{ln2}{\mu max} \quad (4)$$

where: X = Concentration of parasites at the end of the logarithmic phase; X_0 = concentration of parasites at the beginning of the logarithmic phase; t = time (h); μ_{max} = specific growth rate during the logarithmic phase (h^{-1}); ln 2 = 0.69 when $X/X_0 = 2$; t_g = generation time.

2.7.2. Evaluation of lignin cytotoxicity against promastigote forms of *Leishmania amazonensis*

The evaluation of lignin cytotoxicity was performed against promastigotes of *Leishmania amazonensis* cultivated in the stationary phase (72 h). Promastigotes were seeded at a concentration of 1×10^7 parasites/mL in 96-well plates. Then, lignins dissolved in 0.01 % DMSO were added at different concentrations (6.25–100 μg/mL). Plates were incubated in an atmosphere of 5 % CO_2 at 37 °C for 72 h. The drugs amphotericin B was used as a positive control and the negative control as a culture medium and only cells. After the incubation period, the viability of the parasites was determined by counting in a Neubauer chamber. The experiments were performed in biological and experimental triplicate [12].

The IC_{50} value (Concentration capable of inhibiting cell growth by 50 %) was obtained by calculating the non-linear regression of the curves obtained in the graphs of Percentage of viability *versus* concentration of the lignins under study, using the GraphPad Prism program, version 5.0 for Windows. Furthermore, the selectivity index represented by the ratio between the IC_{50} for promastigotes and the CC_{50} for animal cells was determined.

2.7.3. Ultrastructural evaluation of lignin-treated and non-treated promastigotes

The ultrastructural analyzes are useful to evaluate the effect promoted by different molecules against the parasites. The methodology used in this study was proposed by Silva et al. [12] with few modifications. Promastigote forms of *Leishmania amazonensis* were treated at IC_{50} concentrations for lignins and amphotericin B and without treatment (culture medium and cells) for a period of 72 h.

For the scanning electron microscopy (SEM) tests, the parasites were fixed in a 2 % glutaraldehyde solution and 0.1 M sodium cacodylate buffer for 2 h at room temperature. After fixation, the samples were marked with a solution containing 1 % osmium tetroxide in 0.1 M sodium cacodylate buffer for 1 h at room temperature. The parasites were placed on glass coverslips with 0.01 % poly-L-lysine, dehydrated with a series of ethanol (30 to 100 %) and submitted to the critical point (replacement of ethanol by CO_2) LEICA CPD 030. Then, the samples were metallized with gold and observed in the scanning electron microscope JEOL JSM-6390LV.

For Transmission electronic microscopy (TEM), the fixed parasites were washed and post-fixed for one hour in a solution containing 1 % osmium tetroxide (OsO_4), 0.8 % potassium ferricyanide, 5 mM $CaCl_2$ in sodium cacodylate buffer. After this step, the samples were dehydrated in increasing concentrations of acetone, infiltrated and embedded in EPON (Merck). Ultrathin sections of approximately 70 nm in thickness, obtained on a Leica EMUC6 ultramicrotome (Leica, Wetzlar, Germany), were counterstained in uranyl acetate and lead citrate and examined using the TecNai G2 Spirit TEM transmission microscope (FEI, Hillsboro, USA).

2.8. In vitro assay against trypomastigotes forms of Trypanosoma cruzi

In vitro assays with trypomastigotes of *T. cruzi* were performed according to protocols established by Rosa et al. [19]. *Trypanosoma cruzi* parasites (Tulahuen strain) expressing the *Escherichia coli* β-galactosidase gene were cultured on a monolayer of mouse fibroblasts. Cultures were grown in RPMI 1640 medium (pH 7.2–7.4) phenol red plus 10 % fetal bovine serum and glutamine (2 mM). Fibroblasts were seeded into a 96-well tissue culture microplate at a concentration of 4.0×10^3 per well in a volume of 80 μL and incubated overnight. Trypomastigotes expressing β-galactosidase were then added at a concentration of 4.0×10^4 per well in a volume of 20 μL. After 2 h, the medium containing trypomastigotes that did not penetrate the cells was discarded and replaced with 200 μL of fresh medium. After 48 h, the medium was again discarded and replaced by 180 μL of fresh medium with the lignins and the benznidazole standard at different concentrations (6.25–100 μg/mL). After 7 days of incubation, reagents Chlorophenol red-β-D-galactopyranoside (CPRG) (final concentration of 100 μM) and Nonidet P-40 (final concentration of 0.1 %) were added to the plates, followed by overnight incubation at 37 °C. Absorbance was measured at 570 nm in an automated microplate reader. Benznidazole was used as a positive control. The results were expressed as the percentage of growth inhibition for 50 % of the parasites (IC_{50}). Quadruplicates were performed on the same plate and the experiments were repeated at least twice.

2.9. In vitro schistosomicidal activity

2.9.1. Ethical considerations, animals and infection of mice

The study was approved by the UFPE Animal Ethics Committee (n° 0060/2019 CEUA/UFPE). Female Swiss webster mice (*Mus musculus*) with 30 days of age, weighing 30 g (±2 g) were provided and maintained in the vivarium of the Keizo Asami Immunology Laboratory (LIKA/UFPE). Mice ($n = 10$) were infected percutaneously with 80 cercariae of the BH strain of *S. mansoni*. The strain was maintained in the Laboratory of Experimental Schistosomiasis at LIKA/UFPE, through successive passages in *Biomphalaria glabrata* and *Swiss mice*.

2.9.2. In vitro susceptibility of the S. mansoni parasite

The experiments were carried out according to Pereira et al. [20] with modifications. Sixty days after infection, the mice were euthanized by cervical dislocation and the worms aseptically retrieved by perfusion with sterile saline (0.9 % w/v NaCl) of the hepatic portal system and mesentery vessels. The collected worms were immediately transferred to Petri dishes with RPMI 1640 culture medium, supplemented with 20 mM HEPES, 100 μg/mL penicillin, 100 μg/mL streptomycin and 10 % fetal bovine serum, and washed twice with this medium. Subsequently, the worms were distributed (two couples per well) in sterile culture plates with 24 wells of 35 mm in diameter, containing 2 mL of the same supplemented medium. Then, the worms were incubated at 37 °C in a humid atmosphere containing 5 % CO_2. Two hours after incubation, to allow the worms to adapt, lignins were added at final concentrations of 25, 50, 100, 200 and 400 μg/mL. The group Negative Control 1 was formed by couples of worms incubated in supplemented RPMI and in the Negative Control 2 the couples were incubated in RPMI supplemented with 1 % DMSO. Praziquantel at a dose of 10 μM used as standard drug, positive control. All experiments were performed in quadruplicate ($n =$ 8 pairs of worms per concentration) and repeated at least twice.

2.9.3. Viability test

The viability of *S. mansoni*, after treatment, was determined by the cytotoxicity assay based on 3-(4,5-dimethylthiazol-2-yl)-2,5-diphenyltetrazolium (MTT). Briefly, a couple of worms, per well, were distributed in 96-well culture plates and 100 μL of MTT (5 mg/mL in phosphate-buffered saline, PBS) were added and then incubated at 37 °C for 30 min. Then, the MTT solution was replaced by 200 μL of DMSO to dissolve the formazan crystals and the optical density was measured at 550 nm in a microplate reader (M680, from Bio-RadLaboratories, Inc.). This procedure was performed with the worms of the negative control and positive control under the same experimental conditions. This procedure was performed in quadruplicate and repeated twice with worms.

2.10. In vitro anti-Plasmodium falciparum activity

The anti-*plasmodium* assays were performed according to the methodology proposed by Araujo et al. [13] with few modifications. The lignins and tested standards were solubilized in DMSO at 1 %, and serial dilutions 1:3 were performed seven times in RPMI medium supplemented with Albumax I®, with the initial concentration of lignins and chloroquine being 1000 ng/mL (10 μg/mL). *Plasmodium falciparum* 3D7 culture was added to 96-well plates with 3 % parasitemia and 3 % hematocrit, and the lignins and chloroquine were serially diluted in complete RPMI medium. After dilution, the plate was incubated for 72 h at 37 °C. Parasite growth was monitored by flow cytometry, through detection of depolarization (detection of hemozoin) and detection of emitted fluorescence (DNA labeled with SYBR® Green). The tests were carried out in triplicate and the antimalarial activity was defined by the suppression of growth of the parasites treated with lignins in relation to the untreated control and the concentration that inhibits 50 % of the parasite growth (IC_{50}). Assays for the parasite *Plasmodium falciparum* (Dd2) were described under the same conditions previously performed. However, dihydroartemisinin was used as a standard.

2.11. Preliminary evaluation of lignins as excipient for controlled release of benznidazole

2.11.1. Preparation and characterization of tablets

Tablet formulation was carried out according to the methodology proposed by Pishnamazi et al. [21] as few modifications. For this, two formulations were made, the first containing 5 % by weight of the drug (benznidazole), 20 % by weight of lactose, 20 % by weight of lignin, 3 % by weight of croscarmellose sodium and 1 % by weight of magnesium stearate. and 51 % microcrystalline cellulose. The second was composed of without lignin using 71 % of crystalline cellulose and the other constituents in the same proportions previously described. Tablets were produced using a single benchtop punch press (CPR 1) where 500 mg of the different formulations were pressed to make tablets in a 6 mm (diameter) die. Tablet compression was carried out at a speed of 180 mm/min under a fixed load of 400 kg.

The hardness test determines the mechanical resistance of tablets to crushing or rupture under radial pressure. This test was carried out using an Erweka Durometer - Model TBH310 MD equipment using 10 individually tested pills. The disintegration test is the time in which the tablet takes to disintegrate, a state that is defined when no residue of the tested units remains on the metallic screen of the equipment. The experiments were performed on a Pharma Test PTZ-DIST-Disintegration Test Instrument (Hainburg, Germany). In each analysis 6 pills were tested.

2.11.2. In vitro dissolution tests

Dissolution tests were performed according to the methodology

proposed by Pishnamazi et al. [21]. Initially, 900 mL of 0.1 mol/L HCl were added to the dissolution tanks, keeping the temperature at 37 ± 0.3 °C at pH = 1.2. The pills were placed in the vats and then stirring devices were used. The system was maintained under agitation at 50 rpm for 30 min. After this period, a 15 mL aliquot was collected, filtered through standard filter paper, diluted in 50 mL flasks. This experiment was carried out to evaluate the stability of the system. Then the same procedure was carried out for times from 5 to 120 min in order to evaluate the release kinetics. Samples were filtered through 0.22 μm filters and analyzed by high performance liquid chromatography.

2.11.3. Determination of drugs evaluated by high performance liquid chromatography

Benznidazole quantification was performed according to the methodology proposed by Silva et al. [22]. The chromatographic conditions were: C-18 column (12.5 cm × 4 mm id; 5 μm particle), acetonitrile: water (50:50 v/v) mobile phase, flow rate 1 mL/min, UV detector 316 nm, oven temperature 25 °C and injection volume of 20 μL. benznidazole has a retention time of 1.903 min.

2.12. Statistical analysis

Results were expressed as mean ± standard deviation. Statistical evaluation was performed using analysis of variance (ANOVA) for multiple comparisons, followed by Tukey's post-test. Values of $p < 0.05$ were considered significant. The program used to perform the statistical analysis was GraphPad Prism, version 5.0 for Windows.

3. Results and discussion

3.1. Analysis of composition from branches and leaves of Protium puncticulatum and Scleronema micranthum species

The analysis of the composition of branches and leaves is related to the determination of the contents of polysaccharides, lignin, extractives and ash. Table 1 presents the results of the composition analysis in percentage, for the constituent's cellulose, hemicellulose, lignin, extractives and ash for the branches and leaves of *Protium puncticulatum* (PPB and PPL), and *Scleronema micranthum* (SMB and SML) respectively.

As expected, the composition values presented in Table 1 are different between species and between regions, ie, twig or leaf. In the literature, we found few works that report the composition values for the species in this study. Among these, we can mention those carried out by Araújo [23] who obtained the following contents for *Protium puncticulatum* wood: cellulose (39 %), lignin (27.88 %), extractives (7.28 %) and ash (0.27 %). Nascimento et al. [24] obtained the following contents for *Scleronema micranthum* wood: cellulose (53.30 %), lignin (32.32 %), extractives (7.43 %) and ash (1.19 %). Knowing the contents of each constituent is an important step for possible applications.

3.2. Physical and chemical characterization of lignins

3.2.1. Obtaining yield and elemental analysis

Table 2 presents the results of obtaining the yield (after acid precipitation) and the carbon (C), hydrogen (H), nitrogen (N) and oxygen (O) contents for each of the lignins, branches and leaves of *Protium puncticulatum* (PPB and PPL) and *Scleronema micranthum* (SMB and SML).

Table 2
Yield of obtaining and results of elemental analysis with the contents of carbon (C), hydrogen (H), nitrogen (N) and oxygen (O), for lignins obtained from the branches and leaves of *Protium puncticulatum* (PPB and PPL) and *Scleronema micranthum* (SMB and SML) respectively.

Lignins	Obtaining yield (%)	C (%)	H (%)	N (%)	O (%)
PPB	73.4 ± 0.1	60.95 ± 1.0	6.29 ± 0.2	0.13 ± 0.01	32.63 ± 0.1
PPL	63.1 ± 1.2	59.73 ± 1.2	7.32 ± 0.1	0.24 ± 0.01	32.71 ± 1.1
SMB	67.9 ± 1.1	61.46 ± 0.1	7.18 ± 0.3	0.33 ± 0.07	31.03 ± 1.0
SML	60.2 ± 0.3	58.14 ± 0.5	6.20 ± 0.1	0.52 ± 0.01	35.14 ± 0.9

Mean ± Standard Deviation.

The yield results presented in Table 2 showed variations; however, higher yields were observed for the lignins of the branches when compared to the yields obtained for the leaves. This fact may be related, in addition to the different species, to the higher lignin content in the branches. The literature presents different yield results for obtaining lignins. Arruda et al. [10], Silva et al. [12] and Araújo et al. [13] obtaining lignins from the leaves of *Crataeva tapia*, *Morinda citrifolia* and the branches and leaves of *Buchenavia viridiflora* by the same extraction method of this study, that is, acid pre-treatment followed by alkaline delignification and acid precipitation of the lignin obtained yields of 85, 7 %, 89.9 %, 67.9 ± 1.1 % and 60.2 ± 0.3 %, respectively.

The results of the composition analysis showed that the lignins from the branches had higher carbon contents and lower oxygen contents. The hydrogen content for lignin in the branches of *Protium puncculatum* was lower when compared to the leaves. Regarding *Scleronema micranthum* lignins, the branches had higher levels when compared to the leaves. These results are related to the chemical structure of lignins. Nitrogen contents were <1.5 %, this low value indicates that the lignin structure has low levels of contaminants.

These elemental analysis results can be compared to other alkaline lignins. Values close to ours were obtained by Silva et al. [12] for the lignins of the leaves of *Morinda citrifolia* obtained carbon (63.30 ± 1.3 %), oxygen (30.54 ± 0.5 %), hydrogen (5.79 ± 0.1 %) and nitrogen (0.34 ± 0.02 %). Arruda et al. [10] for lignins from *Crataeva tapia* leaves obtained carbon (67.60 %), oxygen (27.18 %), hydrogen (5.101 %) and nitrogen (0.12 %). Araújo et al. [13] evaluating lignin from branches and leaves of *Buchenavia viridiflora*, obtained carbon (61.46 ± 0.1 %), hydrogen (7.18 ± 0.3 %), nitrogen (0.33 ± 0.07 %) and oxygen (31.03 ± 1.0 %) for twig lignin. As for the lignin of the leaves, carbon (58.14 ± 0.5 %), hydrogen (6.20 ± 0.14 %), nitrogen (0.52508 ± 0.01 %) and oxygen (35. 14 ± 0.9 %).

3.2.2. Fourier transform infrared spectroscopy (FTIR) and ultraviolet visible spectroscopy (UV–Vis)

FTIR analysis was applied in order to determine the main functional groups present in the chemical structures of lignins obtained from branches and leaves of *Protium puncticulatum* (PPB and PPL), and *Scleronema micranthum* (SMB and SML) respectively. The spectra were

Table 1
Analysis of the composition for lignins obtained from branches and leaves on a dry basis, together with the material balance.

Samples	Cellulose (%)	Hemicellulose (%)	Lignin (%)	Extractives (%)	Ashes (%)	Total (%)
PPB	30.80 ± 0.2	21.56 ± 0.1	29.85 ± 0.8	13.03 ± 0.0	4.50 ± 0.2	99.74 ± 0.2
PPL	24.10 ± 0.4	19.86 ± 0.9	28.27 ± 0.2	20.37 ± 0.6	6.97 ± 0.0	99.57 ± 0.5
SMB	32.29 ± 0.3	13.66 ± 0.1	34.18 ± 0.4	14.69 ± 0.2	4.87 ± 0.9	99.07 ± 0.1
SML	29.78 ± 0.6	18.16 ± 0.6	27.47 ± 0.1	15.26 ± 0.5	8.43 ± 0.3	99.10 ± 2.1

Mean ± Standard Deviation.

recorded at a wave number between 4000 and 500 cm^{-1} shown in Fig. 1. The bands were identified by comparison using bands previously obtained by Santos et al. [9], Arruda et al. [10], Silva et al. [12] and Araújo et al. [13] featuring different lignins.

According to the spectra presented, characteristic bands present in the chemical structures of lignins can be observed. Thus, an absorption band was identified in the region of acute stretching, in the range of 3600–3200 cm^{-1}, referring to the presence of hydroxyl groups (—OH). The region at 2940–2900 cm^{-1} refers to the presence of asymmetric C—H stretching in methyl and methylene groups. The bands between 1709 and 1700 cm^{-1} refer to the stretching of the carboxylic group (C═O) in unconjugated ketones, carboxylic acids and aldehydes. The bands between 1603 and 1618 cm^{-1} are attributed to symmetrical stretching in aromatic rings in conjunction with C═O stretching. In the region at 1512–1522 cm^{-1} there are bands referring to asymmetric stretching in aromatic rings. The bands between 1451 and 1456 cm^{-1} are attributed to asymmetric deformation of C—H in methyl/methylene. At 1360 to 1367 cm^{-1} there is asymmetric deformation of C—H in CH_3. In the region from 1220 to 1240 cm^{-1} there is stretching at C—C, C—O and C═O. The bands between 1160 and 1165 cm^{-1} are attributed to C═O stretching in conjugated esters. The bands found in the region between 1120 and 1125 cm^{-1} refer to the aromatic ring (typical of syringyl). The bands between 1035 and 1040 cm^{-1} and referring to the C—H deformation in guaiacyl together with C—O deformation in primary alcohols and symmetrical stretching in C—O—C, in addition, this region reveals that these lignins have higher contents of guaiacyl units when compared to syringyl units. In the region between 870 and 875 there is the out-of-plane C—H deformation in *p*-hydroxyphenyl rings. Table 3 presents the assignments for the bands obtained for the lignins of the branches and leaves of *Protium puncticulatum* (PPB and PPL), and *Scleronema micranthum* (SMB and SML).

Spectroscopy in the UV–Vis region is an important technique that helps in the evaluation of the aromatic nature of lignin, through which it is possible to determine the presence of coniferyl (guaiacyl - type G), coumarin (*p*-hydroxyphenyl - type H) and synapyl alcohols. (Syringyl – type S) however, we were unable to predict the chemical structures [9–13]. Therefore, the maximum absorption peak of the UV/Vis spectrum is generally found around 280 nm, corresponding to the electronic transition π - > π* in the aromatic ring, typical of lignins. This bathochromic shift shows a high content of G units [13]. S-type lignins present absorption maximums in the region of 268–276 nm. The absorption that occurs at 310–320 nm is indicative of the presence of H-type units and at 350 nm the absorption of —CH═CHCOOH units occurs [9,11,12,13].

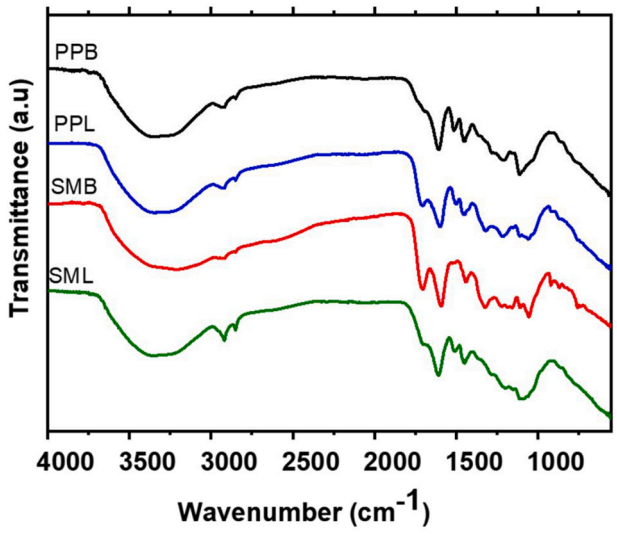

Fig. 1. Spectrum in the infrared region the different alkaline lignins obtained from the branches and leaves of *Protium puncticulatum* (PPB and PPL), and *Scleronema micranthum* (SMB and SML) respectively.

Table 3
Attributions of the bands present in the infrared for the lignins obtained from the branches and leaves of *Protium puncticulatum* (PPB and PPL), and *Scleronema micranthum* (SMB and SML) respectively.

PPB Band (cm^{-1})	PPL Band (cm^{-1})	SMB Band (cm^{-1})	SML Band (cm^{-1})	Vibration	Attribution
3463	3448	3472	3449	st O—H	Phenolic OH + aliphatic OH
2910	2915	2915	2925	st C-H	CH_3—CH_2
2855	2854	2845	2840	st C—H	CH_3—CH_2
1702	1703	1702	1702	st C═O	C═O unconjugated ketones
1603	1618	1611	1608	st C═O	C═O conjugated ketones(S)
1512	1517	1515	1522	st C—C	aromatic ring vibration (G > S)
1451	1456	1454	1451	δasymmetric C—H	CH_3—CH_2
1365	1367	1365	1360	δasymmetric C—H	CH_3
1238	1225	1220	1220	st C═O	(G)
1160	1161	1161	1163	st C═O	C═O in conjugated esters
1124	1126	1122	1129	δ_{op} Ar C–H	(S)
1040	1042	1039	1040	δ_{ip} Ar C–H	G > S
870	875	875	871	δ_{op} Ar C–H	(H)

Guayacyl (G), Syringyl (S) and *p*-hydroxyphenyl (H), st: stretching vibration, δ_{ip} In-plane deformation vibration, δ_{op}: Out-of-plane deformation vibration.

Fig. 2A shows the spectra of lignins obtained from the branches and leaves of *Protium puncticulatum* (PPB and PPL), and *Scleronema micranthum* (SMB and SML). In addition, Fig. 2B shows the concentration lines as a function of absorbance to obtain the extinction coefficient.

The results obtained in Fig. 2 were compared to those obtained Santos et al. [9], Melo et al. [11], Silva et al. [12] and Araújo et al. [13]. The lignins in this study showed a similar profile in relation to the UV/Vis spectra. The band between 250 and 280 nm is related to chromophore groups of conjugated and unconjugated phenolic compounds, in addition, the maximum absorbance having occurred at 280 nm, confirms as well as in the FTIR that there is a greater amount of guaiacyl-type units in syringyl groups would have the closest band at 270 nm. In addition, the lignins showed a discrete band at 350 nm referring to the presence of hydrocinnamic acids.

Table 4 presents the values of maximum wavelength, equation of the line and absorptivity for the lignins obtained from the branches and leaves of *Protium puncticulatum*, and *Scleronema micranthum*.

Table 5 presents the absorptivity values obtained by other authors evaluating different lignins using the same process of obtaining acid pretreatment followed by alkaline delignification. These differences are associated, in addition to the type of lignin, that is, source of production, the degree of condensation and substitution of these lignins. The greater the number of substituted rings, the greater the absorptivity at 280 nm [9–13].

Spectroscopy in the UV–Vis region is an important technique that helps in the evaluation of the aromatic nature of lignin, through which it is possible to determine the presence of coniferyl (guaiacyl - type G), coumarin (*p*-hydroxyphenyl - type H) and synapyl alcohols. (Syringyl – type S) however, are not able to predict the chemical structures [9–13]. Therefore, the maximum absorption peak of the UV/Vis spectrum is generally found around 280 nm, corresponding to the electronic transition π - > π* in the aromatic ring, typical of lignins. This bathochromic shift shows a high content of G units [13]. S-type lignins show absorption maxima in the region of 268–276 nm. The absorption that occurs at 310–320 nm is indicative of the presence of H-type units and at 350 nm the absorption of —CH═CHCOOH units occurs [9,11,12,13].

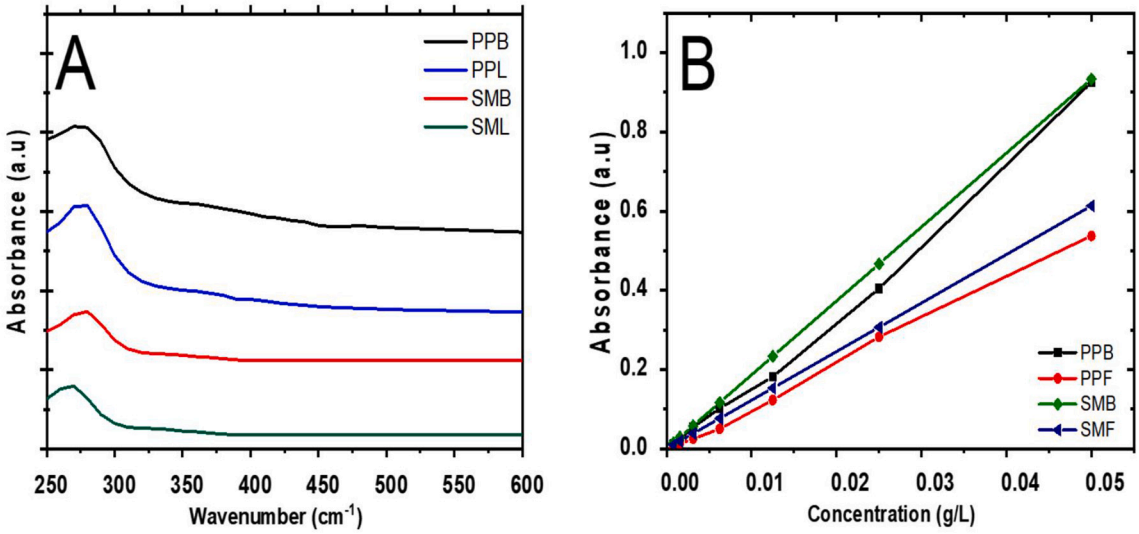

Fig. 2. Spectrum in the UV/vis region (A) and the curves for the determination of the absorptivity (B) for the lignins of the branches and leaves of *Protium puncticulatum* (PPB and PPL), and *Scleronema micranthum* (SMB and SML) respectively.

Table 4
Maximum absorption length and straight-line equation for lignins from branches and leaves of *Protium puncticulatum* and *Scleronema micranthum*.

Lignins	Max wavelength (cm^{-1})	Line equation
Protium puncticulatum branches	284	$y = 18.363\times - 0.017$; $R^2 = 0.9947$
Protium puncticulatum leaves	282	$y = 10.997\times - 0.0077$; $R^2 = 0.998$
Scleronema micranthum branches	282	$y = 19.667\times + 6E\text{-}17$; $R^2 = 0,993$
Scleronema micranthum leaves	281	$y = 15.267\times + 6E^{-}17$; $R^2 = 0.997$

Table 5
Values of the extinction coefficient for lignin from branches and leaves of *Protium puncticulatum*, and *Scleronema micranthum* compared to values obtained by different lignins.

Lignin	Absorptivity (L/g/cm)	References
Protium puncticulatum branches	18.36	This work
Protium puncticulatum leaves	10.99	This work
Scleronema micranthum branches	19.66	This work
Scleronema micranthum leaves	15.26	This work
Caesalpinia pulcherrima leaves	22.27	Melo et al. [11]
Crataeva tapia leaves	12.8	Arruda et al. [10]
Morinda citrifolia leaves	16.7	Silva et al. [12]
Buchenavia viridiflora branches	18.66	Araújo et al. [13]
Buchenavia viridiflora leaves	12.27	Araújo et al. [13]

3.2.3. Characterization by Nuclear Magnetic Resonance (HSQC NMR)

Fig. 3 presents the HSQC spectra for the lignins obtained in this study. The signals were previously assigned by Silva et al. [12] and Araújo et al. [13] evaluating different alkaline lignins.

The signals obtained in the aliphatic region (δ_C/δ_H10.0–40.0/0.50–2.50 ppm) were attributed to methyl groups (CH_3—) belonging to acetyl groups. This signal was found only in the lignins of the branches of *Protium puncticulatum* (Fig. 3A) and *Scleronema micranthum* (Fig. 3C).

Regarding the signals referring to the side chain (δ_C/δ_H 50.0–95.0/2.50–6.00 ppm) only the lignins of the branches showed Cβ–Hβ signals in phenylcoumaran (Bβ) substructures (Fig. 3A and C). Methoxyl groups (—OCH_3) were found in all lignins in this study. Twig lignin (Fig. 3A and C) and leaf lignin of *Scleronema micranthum* (Fig. 3D) showed signs of Cγ–Hγ in β-O-4′ (A) (Aγ) substructures. The signals referring to Cγ–Hγ in β-O-4′ (A') substructures were found only in the lignins of the leaves of *Protium puncticulatum* (Fig. 3B) and in the lignin of the twig of *Scleronema micranthum* (Fig. 3C). the signals referring to Cγ–Hγ in β-O-4′ (A") substructures, Cα–Hα in the β-aryl ether substructure and C5-H5 in β-D-xylopyranoside were found only in the lignins of the branches. The signal referring to Cα–Hα in acetylated β-aryl ether was found only in the lignin of the twig of *Protium puncticulatum* (Fig. 3A). The Cβ–Hβ signal in β-O-4′ substructures linked to a G unit was obtained in all lignins with the exception of lignin from the leaf of *Protium puncticulatum* (Fig. B). Finally, in this region, a signal attributed to Cα–Hα) was obtained in phenylcoumaran substructures present only in the lignins of the branches (Figs. A and C).

In the aromatic region (δ_C /δ_H 95.0–150.0/5.50–8.00 ppm), it was possible to observe characteristic signals present in the G, S and H units present in the lignin structures in addition to signals. These results reinforce that the lignins in this study are of the GSH type with a predominance of G units.

Table 6 presents the main δ_C/δ_H correlations and assignments performed through the $^1H^{13}C$ HSQC spectra.

3.2.4. Molecular weight determination by gel permeation chromatography (GPC)

Table 7 presents the results obtained by the GPC for the lignins of the branches and leaves of *Protium puncticulatum* (PPB and PPL) and *Scleronema micranthum* (SMB and SML) compared to other molecular weight results for different lignins using the same production process, Acid pretreatment followed by alkaline delignification.

The results obtained were close to those obtained by other authors characterized different lignins. The values presented in Table 7 shows that the lignins of the branches presented higher values of numerical average mass (Mn) and weighted average molar mass (Mw) when compared to the lignins of the leaves. Lignins with lower molecular weight are more reactive because they have higher levels of phenolic and aliphatic hydroxyls, suggesting that in the extraction process there were cleavages of ether-type bonds to structures of lower molecular weight. The low polydispersity values show that these lignins present fragments with low heterogeneity in terms of molecular weight [13]. In addition, the lignins in this work are classified as having low molecular weight, presenting values of <4000 Da [9–13].

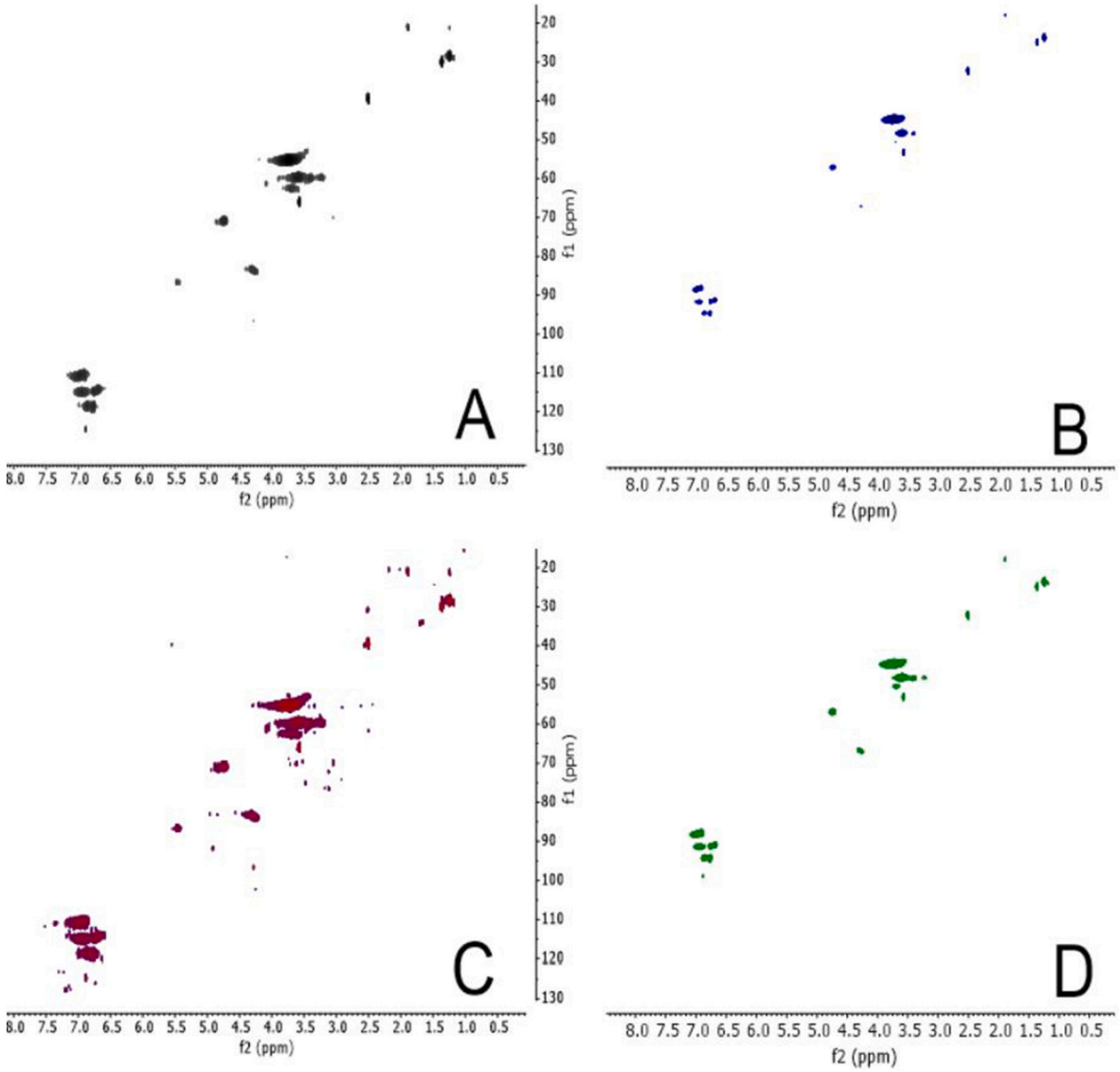

Fig. 3. Spectrum HSQC NMR spectra for the different alkaline lignins obtained from branches (A) and leaves (B) of *Protium puncticulatum*. Lignin spectra of branches (C) and leaves (D) of *Scleronema micranthum* respectively.

3.2.5. Thermal analysis: thermogravimetric (TG), derived thermogravimetric (DTG) and differential scanning calorimetry (DSC) and fast pyrolysis in Py-GC/MS

Thermogravimetric analysis has been widely used in the study of thermal stability and physicochemical characterization of lignins, as reported in studies carried out by, Silva et al. [12] and Araújo et al. [13]. The thermal degradation of lignins is quite complex, because different chemical bonds present in their macromolecular structure are broken during the increase in temperature [12]. In addition, different works report that lignins have a wide range of thermal degradation temperatures. Which varies from temperatures ranging from 20 to 800 °C [12,13].

Fig. 4 shows the curves obtained by thermogravimetric analysis (TGA), and the DTG curves (thermogravimetric derivative). For the lignins obtained from the branches and leaves of *Protium puncticulatum* (PPB and PPL), and *Scleronema micranthum* (SMB and SML) respectively.

The lignins presented different thermal behavior, the two lignins of the branches presented three prominent thermal events, whereas the lignins of the branches presented two events, which were confirmed by the DTG curves (Fig. 4B). The attributions for each of the events were previously identified by Arruda et al. [9], Melo et al. [11], Silva et al. [12] and Araujo et al. [13] evaluating the thermal behavior of different lignins.

Thus, the events found were: the first found before 100 °C, related to the loss of water molecules by evaporation (event found in all lignins in this study). An event between 250 °C and 315 °C was observed for branch lignins, where mass loss occurs, resulting in non-lignin compounds, such as polysaccharides and alcohols and aliphatic acids, in addition to the cleavage of β-O-4 bonds. In the region between 300 and 420 °C, this event is related to the breaking of the characteristic bonds (β-O-4′ and β-β, for example) that connect the structural units of lignins (an event found in all lignins in this study). Finally, at temperatures above 450 °C, no significant variations in mass loss were observed.

Table 8 presents the mass loss in percentage for each of the events presented. For the lignins obtained from the leaves and branches of *Protium puncticulatum* (PPB and PPL) and *Scleronema micranthum* (SMB and SML) respectively.

The DSC curves of the lignins under study can be seen in Fig. 5. The signals were previously identified by Melo et al. [11], Silva et al. [12] and Araújo et al. [13] evaluating lignins obtained from different sources, namely: alfalfa, flax fiber, pine straw, leaves and branches.

The curves show an endothermic peak that occurs between 0 and

Table 6
Assignments of the signals present in the HSQC NMR spectrum for the lignins obtained from the branches and leaves of *Protium puncticulatum* (PPB and PPL), and *Scleronema micranthum* (SMB and SML) respectively.

Lables	PPB δ_C/δ_H (ppm)	PPLδ_C/δ_H (ppm)	SMB δ_C/δ_H (ppm)	SML δ_C/δ_H (ppm)	Assignments
CH_3-	20.4/ 1.88–1.93	–	20.4/ 1.88–1.93	–	CH_3-) in acetyl group
B_β	53.2/3.57	–	53.2/3.57	–	(C_β–H_β) in phenylcoumaran substructures
-OCH_3	55.6/3.73	55.6/ 3.73	55.6/3.73	55.6/3.73	(C-H) in methoxy
Aγ	60.0–60.8/ 3.59–3.69	–	60.0–60.8/ 3.59–3.69	60.0–60.8/ 3.59–3.69	(C_γ–H_γ) in β-O-4′ substructures (A)
A'γ	–	63.3/ 3.96	63.3/3.96	–	(C_γ–H_γ) in β-O-4′ substructures (A')
A"γ	62.0/ 4.1–4.2	–	62.0/ 4.1–4.2	–	(C_γ–H_γ) in β-O-4′ substructures (A")
Aα(G)	71.3/4.74	–	71.3/4.74	–	(C_α–H_α) in β-aryl ether substructure
X5	64.28/ 3.57	–	64.28/ 3.57	–	(C_5-H_5) in β-D-Xylopyranoside (X)
A'α	71.2/4.87	–	–	–	(C_α–H_α) in β-aryl ether acetylated
Aβ(G)	83.6/4.30	–	83.6/4.30	83.6/4.30	(Cβ–Hβ) in β-O-4′ substructures linked to a G unit (A)
Bα	86.9/5.55	–	86.9/5.55	–	(C_α–H_α) in phenylcoumaran substructures
PhGly	–	–	101.6/ 4.90	–	phenylglycoside bond
S′2.6	107.0/7.1	107.0/ 7.1	107.0/7.1	107.0/7.1	($C_{2.6}$-$H_{2.6}$) in oxidized (Cα = O) phenolic syringyl units (S′)
G_2	110.9/ 6.99	110.9/ 6.99	110.9/ 6.99	110.9/ 6.99	(C_2–H_2) in guaiacyl units
FA_2	–	–	–	110.7/ 7.30	(C_2–H_2) in ferulic acid
H $_{3.5}$	114.9 / 6.7	114.9 / 6.7	114.9 / 6.7	114.9 / 6.7	($C_{3.5}$ – $H_{3.5}$) in H-units
G_6	118.7/ 6.77	118.7/ 6.77	118.7/ 6.77	118.7/ 6.77	(C_6–H_6) in G-units
$H_{2.6}$	–	–	127.8/ 7.22	–	($C_{2.6}$–$H_{2.6}$) in H-units

A: *β-O-4′* linkages; B: resinol structures (*β-β′*); G: guaiacyl units; S: syringyl units; X:Xylopyranoside; H: *p*- hydroxyphenyl.

100 °C, this peak may be related to the loss of adsorbed water in the sample. Between 350 and 450 °C we have superimposed exothermic peaks, related to processes occurring in the lignin pyrolysis reaction. These signals corroborate those obtained by the TGA/DTG curves.

During pyrolysis, lignin is fragmented through thermal energy, in an inert atmosphere, producing a mixture of aromatic compounds [13]. These compounds are easily separated by gas chromatography and identified by mass spectrometry [12,13]. Based on the degradation products, lignin can be characterized in terms of *p*-hydroxyphenyl (H), syringyl (S) and guaiacyl (G) units, since the substitution pattern present in its original structure is maintained [12]. The mechanism of lignin degradation was previously described in the results of thermogravimetric analysis [12,13].

For this pyrolysis, the use of a pyrolysis temperature of 550 °C was defined, as it is the most suitable temperature for the pyrolytic behavior of the lignins under study. This temperature was confirmed by TGA/DTG thermal analysis. In addition, other authors also use this same temperature to characterize different lignins Silva et al. [12] and Araújo et al. [13].

Table 7
Molecular distribution results for lignins from branches and leaves of *Protium puncticulatum*, and *Scleronema micranthum* compared to values obtained by different lignins.

Lignins	Mw (Da)	Mn (Da)	Mw/ Mn	References
Protium puncticulatum branches	2019.24	1945.40	1.0	This work
Protium puncticulatum leaves	965.59	578.03	1.7	This work
Scleronema micranthum branches	4000	3089.11	1.3	This work
Scleronema micranthum leaves	901.53	498.30	1.8	This work
Caesalpinia pulcherrima leaves	2503	1472	1.7	Melo et al. [11]
Crataeva tapia leaves	1246.8	831.2	1.5	Arruda et al. [10]
Morinda citrifolia leaves	2995	1762	1.7	Silva et al. [12]
Conocarpus erectus leaves	2709	1279	2.1	Santos et al. [9]
Buchenavia viridiflora branches	3945.10	2000.92	2.0	Araújo et al. [13]
Buchenavia viridiflora leaves	984.77	691.50	1.4	Araújo et al. [13]

Fig. 6 shows the chromatograms obtained during pyrolysis for the lignins obtained in our study.

The chromatograms present very similar profiles, the difference between them is directly related to the intensity of the signals. Table 8 presents the compounds and relative area values of the sample under study. The signs were previously identified by Silva et al. [12] and Araújo et al. [13] characterizing different lignins. Through the results obtained in Table 9, it was possible to determine the estimated percentage of the constituents present in the structure, that is, aromatic (those that are not G, S and H units), catechol and G, S and H units. These results are found in Table 10.

The results presented in Tables 9 and 10 show that the lignins are of the GSH type with predominance in G units. In addition, they present structural differences. Confirming with the results obtained during the spectroscopic analysis.

3.2.6. Using the radar tool to compare lignins

The use of radar charts allows a direct comparison of the different lignins by comparing the key parameters [25,26]. The parameters selected for drawing up the graphs were: β-O-4 bond content (determined by NMR, HSQC), non-condensed units (NCS) (determined by NMR, HSQC; NCS = 100 - condensed units (DC) and G, S and H (by pyrolysis coupled to GC/MS) The graphs were shown in Fig. 7 for each of the lignins.

The radar charts confirm that the lignins isolated structural differences from each other. This shows that the lignins, even being obtained by the same extraction method and from the same plant, present variations when it comes to the region where it is extracted (twig or leaf). The lignins from the leaves (Fig. 7B and D) showed higher levels of β-O-4 and NCS bonds, when compared to the lignins from the branches (Fig. 7A and C). That is, the lignins in the leaves are less condensed. Thus, leaf lignins are more easily removed from the cell wall when compared to twig lignins during the delignification process, in addition to being more easily depolymerized [25,26].

The literature presents some works that use the radar tool to compare lignins. Costa et al. [25] evaluating different Kraft lignins obtained from eucalyptus, mimosa and willow. Costa et al. [26] evaluating lignins from stems and roots of corn, cotton and tobacco obtained by light acidolysis.

These findings show that lignins extracted by different processes and sources have different chemical structures. In our work, the lignins obtained by different regions of the plant, that is, branches or leaves, showed different chemical structures even using the same production process (acid pre-treatment followed by alkaline delignification).

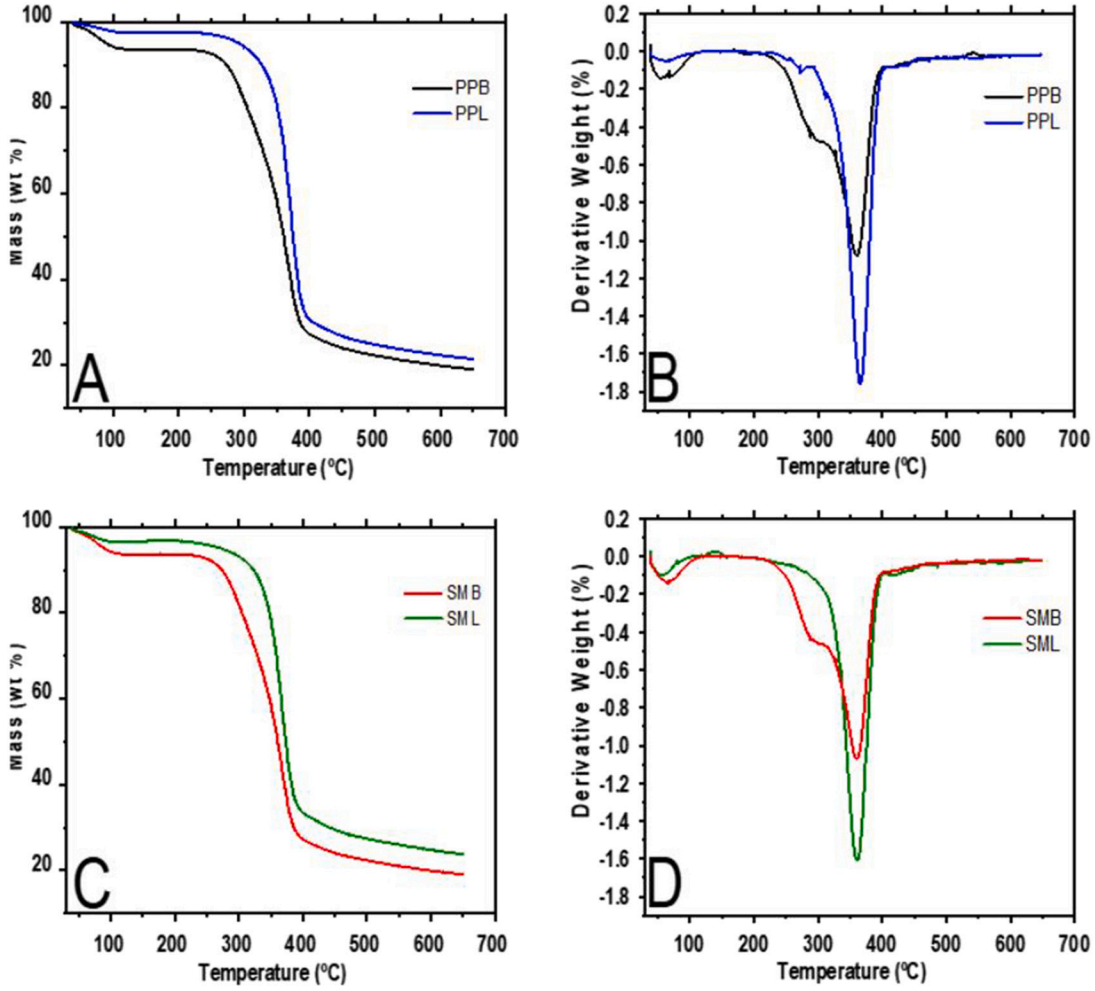

Fig. 4. Thermogravimetric curves (TGA) (A) the first derivative of mass loss (DTG) (B) and for the lignins obtained from the branches and leaves of *Protium puncticulatum* (PPB and PPL). Thermogravimetric curves (TGA) (C) the first derivative of mass loss (DTG) (D) for the lignins obtained from the branches and leaves of *Scleronema micranthum* (SMB and SML) respectively.

Table 8
Mass loss values in percentage for each of the thermal degradation events, maximum degradation temperature obtained by the DTG and percentage of residual mass. For the lignins obtained in this study.

Lignins	T_{P1} (° C)	Mass (%)	T_{P2} (° C)	Mass (%)	T_{P3} (°C)	Mass (%)	Residual mass (%)
PPB	62.5	4.2	289.3	17.3	362.0	59.79	18.71
PPL	61.7	3.4	ND	ND	364.5	75.11	21.49
SMB	67.4	3.9	287.7	16.6	362.7	60.64	18.86
SML	53.7	3.5	ND	ND	360.5	72.71	23.79

T_P: Peak temperature at each degradation event determined by DTG, ND: not determined.

3.3. Evaluation of in vitro antioxidant activity and total phenolic content

The results of the quantification of the phenolic groups present in the chemical structures of the lignins of the branches and leaves of *Protium puncticulatum*, and *Scleronema micranthum* (SMB and SMl), were compared to other authors and are presented in Table 11. The results were expressed in equivalent grams of gallic acid per gram of lignin (GAE/g).

The results presented in Table 11 showed that the lignins in the leaves had higher levels of phenolic groups when compared to the lignins in the branches. This fact is confirmed by the results obtained by elemental, UV/visible as and GPC (low molecular weight) analyses,

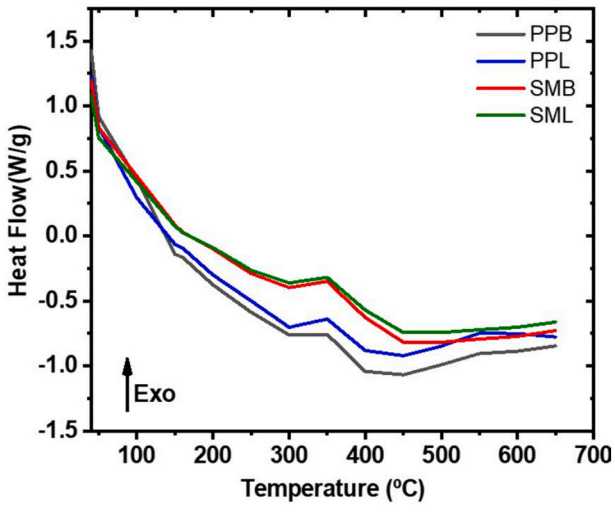

Fig. 5. Differential scanning calorimetry (DSC) analysis curves for the lignins from the branches and leaves of *Protium puncticulatum* (PPB and PPL), and *Scleronema micranthum* (SMB and SML) respectively.

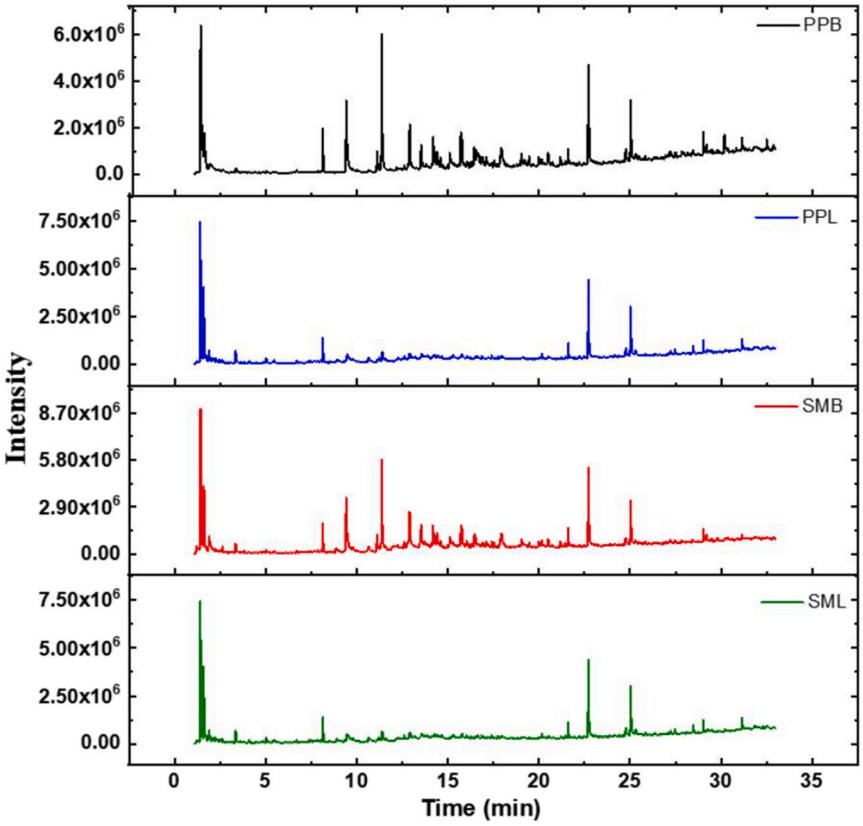

Fig. 6. Chromatograms for lignins from branches and leaves of *Protium puncticulatum* (PPB and PPL), and *Scleronema micranthum* (SMB and SML) respectively.

Table 9
Relative distribution of the peak area of the main products for the lignins obtained from the branches and leaves of *Protium puncticulatum* (PPB and PPL), and *Scleronema micranthum* (SMB and SML) respectively in Py-GC/MS.

RT/ min	Product compounds	Formula	Origin	PPB relative percentage (%)	PPL relative percentage (%)	SMB relative percentage (%)	SML relative percentage (%)
2.3	Benzene	C_6H_6	Aromatic	1.65	1.94	3.61	1.06
3.3	Toluene	C_7H_8	Aromatic	0.89	2.39	6.82	1.11
5.0	xylene	C_8H_{10}	Aromatic	0.78	1.27	2.69	0.53
7.4	Phenol	C_6H_6O	H-lignin	1.22	1.05	12.96	0.68
9.2	4-methylphenol	C_7H_8O	H-lignin	6.66	1.35	2.37	7.43
9.5	Guaiacol	$C_7H_8O_2$	G-lignin	9.91	1.47	4.82	12.36
10.9	4-ethylphenol	$C_8H_{10}O$	H-lignin	3.06	1.94	3.29	3.81
11.4	4-methylguaiacol	$C_8H_{10}O_2$	G-lignin	18.94	23.56	6.22	23.42
11.7	catechol	$C_6H_6O_2$	catechol	11.55	9.42	3.45	1.21
12.7	3-methoxycatechol	$C_7H_8O_3$	catechol	6.77	10.16	4.53	5.02
13.0	4-ethylguaiacol	$C_9H_{12}O_2$	G-lignin	6.98	10.01	5.58	8.01
13.5	4-vinylguaiacol	$C_9H_{10}O_2$	G-lignin	4.49	0.77	5.45	4.87
14.2	Syringe	$C_8H_{10}O_3$	S-lignin	4.81	7.12	5.14	6.28
14.4	4-propylguaiacol	$C_{10}H_{14}O_2$	G-lignin	5.79	5.49	4.53	2.99
15.8	4-(1-propenyl)-guaiacol	$C_{10}H_{12}O_2$	G-lignin	0.52	6.98	5.45	6.61
16.4	Acetovanilone	$C_9H_{10}O_3$	G-lignin	3.61	4.91	4.82	4.44
17.1	3-acetonylguaiacol	$C_{10}H_{12}O_3$	G-lignin	2.63	0.48	5.14	2.70
18.1	4-(2-propenyl)-syringol	$C_{11}H_{14}O_3$	S-lignin	3.93	2.46	4.21	0.45
19.0	Syringaldehyde	$C_9H_{10}O_4$	S-lignin	2.85	3.86	3.61	3.62
19.9	4-ethanoylsyringol	$C_{10}H_{12}O_4$	S-lignin	2.95	3.34	5.31	3.42

RT: Retention time G: guaiacyl units; H: *p*-hydroxyphenyl units; S: syringyl units.

which showed that the lignins in the leaves were more oxygenated and more branched. These branches can promote an increase in the number of phenolic and non-phenolic end groups [12,13]. Furthermore, when comparing other different lignins obtained by the same method of obtaining, it is observed that the results were different. This difference in contents is directly related to the source of obtaining these lignins [8–13].

The phenolic groups present in the lignin structures give this macromolecule an antioxidant character [11–13]. The antioxidant activity of phenolic groups is mainly due to their oxidation-reduction properties, which can play an important role in absorbing and neutralizing free radicals, chelating triplet and singlet oxygen or decomposing

Table 10
Estimated percentage of the main products found for lignins obtained from branches and leaves *of Protium puncticulatum* (PPB and PPL), and *Scleronema micranthum* (SMB and SML) respectively in Py-GC/MS.

	Aromatics (%)	Catecol (%)	H (%)	S (%)	G (%)	TOTAL
PPB	3.3	18.32	10.95	14.54	52.87	100.0
PPL	5.6	19.59	4.34	16.79	53.68	100.0
SMB	13.1	7.98	18.62	18.27	42.01	100.0
SML	2.7	6.22	11.92	13.77	65.40	100.0

G: guaiacyl units; H: *p*-hydroxyphenyl units; S: syringyl units.

peroxides [9–13]. Therefore, due to the presence of these groups, lignins are considered as natural antioxidant agents. Different assays to evaluate the antioxidant activity *in vitro* have been carried out in order to evaluate the antioxidant potential of lignins.

Fig. 8 shows the antioxidant activity curves promoted by the lignins of this study in different assays.

The curves presented in Fig. 8 show that the antioxidant activity increases with increasing concentration. This profile was also observed by Cruz-Filho et al. [8], Santos et al. [9], Melo et al. [11], Silva et al. [12] and Araújo et al. [13]. It can be seen that the results of higher activity were promoted in the DPPH (Fig. 8A) and ABTS (Fig. 8B) radical capture assays. Through the curves it was possible to obtain results numbers of antioxidant activity, these values are presented in Table 12.

The results in the table showed that all lignins in this study promoted promising results of antioxidant activity for the ABTS assay. The most promising lignin is obtained from the branches of *Scleronema micranthum*. The lignin that showed the lowest activity value for this a assay was obtained from the branches of *Protium puncticulatum*. The second assay that presented good results of antioxidant activity was the DPPH radical capture assay, the lignin that presented the highest result for the activity was obtained from the leaves of *Scleronema micranthum* and the lignin that presented the lowest activity results was also the lignin obtained from branches of *Protium puncticulatum*. In relation to the molybdenum and iron reduction assays, the lignins did not present IC_{50} showing very low percentages of activity. Therefore, these lignins present promising results for the ABTS and DPPH radical scavenging assays.

From the results obtained from phenolic groups present in the chemical structure of the lignins of our study and the results of antioxidant activity for the ABTS and DPPH assays, a correlation study between the content of phenolic groups and antioxidant activity was carried out. These results were presented in Fig. 9.

In this study, a low correlation was observed between the variables, content of phenolic groups and antioxidant activity for the lignins under study ($R^2 = 0.00639$; $R^2 = 0.4727$), showing that antioxidant activity is not exclusively due to phenolic groups, but also to other groups functional (activity promoters or not) present in the lignin structure, that is, the conjugated double bonds can promote an additional stabilization of the phenoxyl radicals through prolonged reallocation, which can contribute to the increase of the activity. However, conjugated carbonyl groups and aliphatic hydroxyl groups promote lows. These results confirm the hypothesis that different functional groups present in the lignin structure can contribute to the increase or decrease of antioxidant activity. These results were also reported by Cruz-Filho et al. [8], Santos

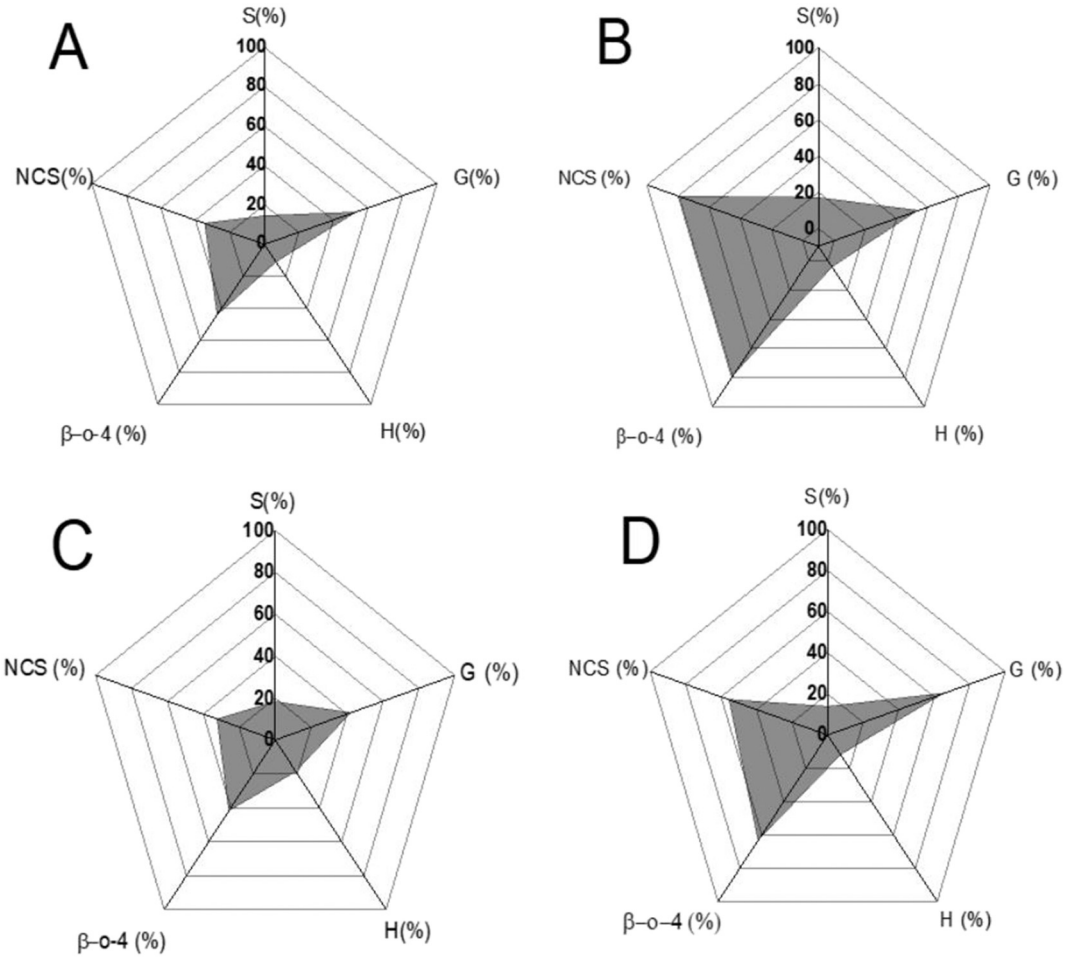

Fig. 7. Radar graph used to compare the lignins obtained from the branches (A) and leaves (B) of *Protium puncticulatum* and for the lignins obtained from the branches (C) and leaves (D) of *Scleronema micranthum* respectively.

Table 11
Results of the determination of phenolic groups present in the lignins obtained in this study and compared to other lignins were expressed in mg of GAE/g.

Lignins	Phenolic content (mg GAE/g)	References
Protium puncticulatum branches	140.411 ± 0.929	This study
Protium puncticulatum leaves	276.624 ± 0.879	This study
Scleronema micranthum branches	237.936 ± 2.533	This study
Scleronema micranthum leaves	166.519 ± 2.171	This study
Caesalpinia pulcherrima leaves	41.33	Melo et al. [11]
Crataeva tapia leaves	189.6	Arruda et al. [10]
Morinda citrifolia leaves	193.3	Silva et al. [12]
Conocarpus erectus leaves	465.90	Santos et al. [9]
Opuntia ficus-indica cladodes	36.4	Cruz-Filho et al. [8]
Opuntia cochenillifera cladodes	87.8	Cruz-Filho et al. [9]
Buchenavia viridiflora branches	237.936	Araujo et al. [13]
Buchenavia viridiflora leaves	166.519	Araujo et al. [13]

Mean ± Standard Deviation.

et al. [9], Melo et al. [11], Silva et al. [12] and Araújo et al. [13] evaluating different lignins.

3.4. Cytotoxicity assays

Table 13 shows the results of cytotoxicity against macrophage cells, fibroblasts, Vero, Hepg2 and hemolytic activity respectively.

The results presented in Table 13 showed that the lignins presented CC_{50} values for J774 macrophages ranging from 34.20 to 48.47 μg/mL, for V79 fibroblasts from 92.85 to 98.23 μg/mL, Vero cells 93.64 to 99 μg/mL, Hepg2 presented higher values than 100 μg/mL. Finally, they presented percentage of hemolysis values lower than 5 %. The literature describes lignins as macromolecules with low cytotoxicity. The different CC_{50} values are related to the type of lignin/chemical structure, production source, cell type, concentration and method used to evaluate the cytotoxic effect.

Silva et al. [12] evaluating the cytotoxic effect promoted by alkaline lignin obtained from *Morinda citrifolia* leaves, obtained a CC_{50} of 31.0 ± 1.10 μg/mL against J774.A1 macrophages. Araújo et al. [13] evaluating the cytotoxic effect of lignins obtained from branches and leaves of *Buchenavia viridiflora* against J774.A1 macrophages, obtained a CC_{50} of 28.47 ± 0.26 μg/mL and 22.58 ± 0.61 μg/mL, respectively. In addition, they verified low cytotoxicity against Hepg2, they were not toxic, they presented CC_{50} values >100 μg/mL and in relation to hemolytic activity, they were not considered as hemolytic agents. These results corroborate that lignins may have low cytotoxicity against different cell types.

3.5. In vitro leishmanicidal activity against promastigote forms promoted by lignins

When performing *in vitro* leishmanicidal assays, different cells can be evaluated, among which we can mention: neutrophils, dendritic cells, macrophages, fibroblasts and epithelial cells [12].

For this, a kinetics of growth of the promastigotes forms in Schneider medium was performed to obtain the parasites in the stationary phase of growth. Fig. 10 presents the results of parasite growth kinetics. Fig. 10A shows all phases, ie logarithmic, exponential, stationary and decay phase. Fig. 10B shows only the exponential phase to determine growth rate and generation time.

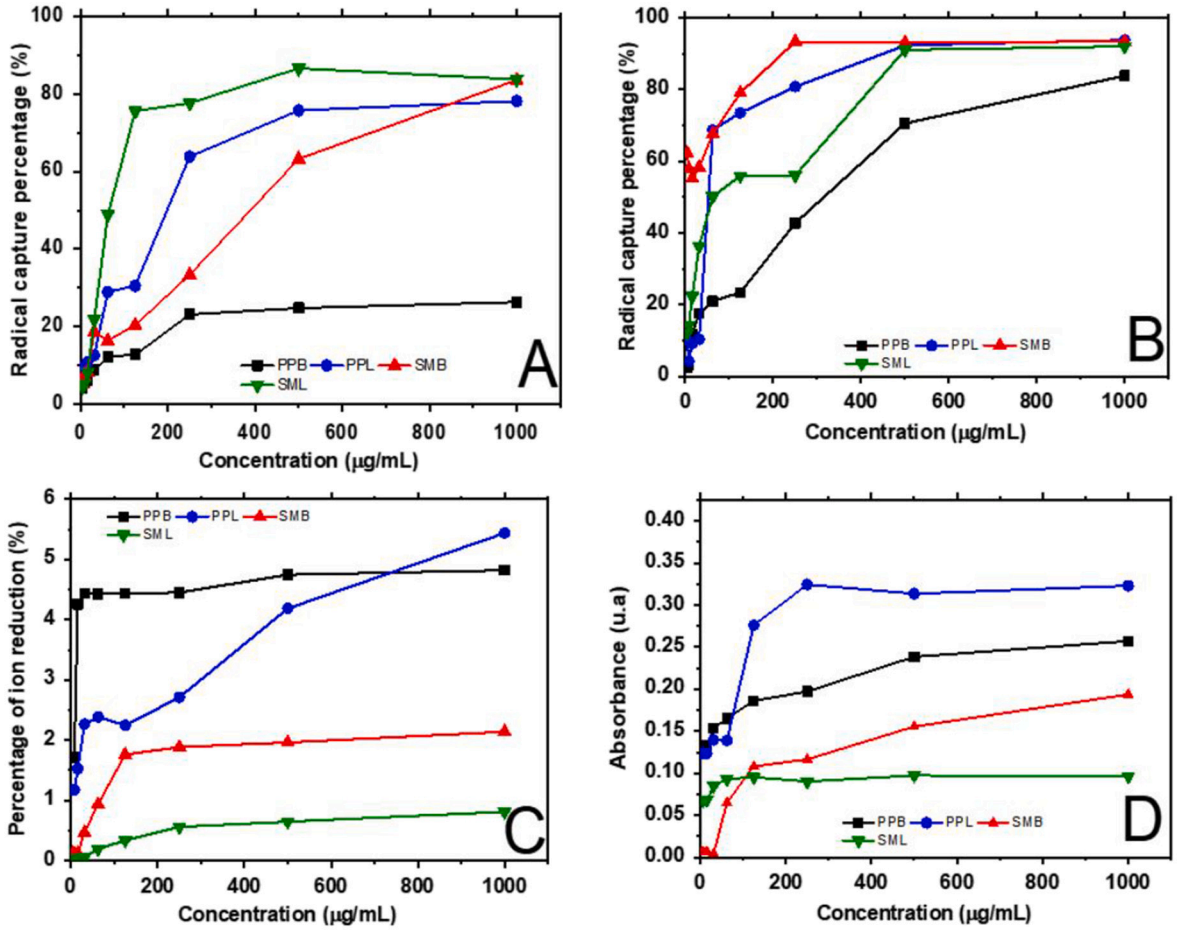

Fig. 8. Antioxidant activity promoted by lignins from branches and leaves of *Protium puncticulatum* (PPB and PPL), and *Scleronema micranthum* (SMB and SML) respectively. By different tests. Capture of DPPH (A), ABTS (B) radicals and reduction of molybdenum (C) and iron (D) ions.

Table 12
Antioxidant activity promoted by lignins from branches and leaves of *Protium puncticulatum* (PPB and PPL), and *Scleronema micranthum* (SMB and SML) by the following assays: capture of DPPH and ABTS radicals and reduction of molybdenum and iron ions.

Lignins	*Radical DPPH•*		Radical ABTS +		Reduction $Mo^{6+} - Mo^{5+}$		Reduction Fe^{3+}- Fe^{2+}	
	% Radical capture at 1000 μg/mL	EC_{50} (μg/mL)	% Radical capture at 1000 μg/mL	EC_{50} (μg/mL)	% Radical capture at 1000 μg/mL	EC_{50} (μg/mL)	% Radical capture at 1000 μg/mL	EC_{50} (μg/mL)
PPB	25.35 ± 0.1	Nd	83.84 ± 1.37	455.37 ± 0.9	4.8 ± 0.0	ND	25	ND
PPL	78.12 ± 0.2	252.72 ± 0.3	93.81 ± 0.0	419.83 ± 1.0	5.4 ± 0.01	ND	32	ND
SMB	83.60 ± 0.19	477.35 ± 1.2	94. 0 ± 0.1	1.4 ± 0.0	2.1 ± 0.02	ND	19	ND
SML	83.72 ± 0.15	77.65 ± 0.4	92.04 ± 0.5	62.5 ± 1.0	0.8 ± 0.03	ND	9	ND
Ascorbic acid	99.8	7.75 ± 0.01	99.0	13.4 ± 0.01	98.0	5.34 ± 0.5	90.0	26.49 ± 0.3
Butylated hydroxytoluene (BHT)	99.1	18.9 ± 0.03	100	5.24 ± 0.02	94.0	8.85 ± 0.1	70.0	5.30 ± 0.1

Mean ± Standard Deviation; ND: not determined at the concentrations studied.

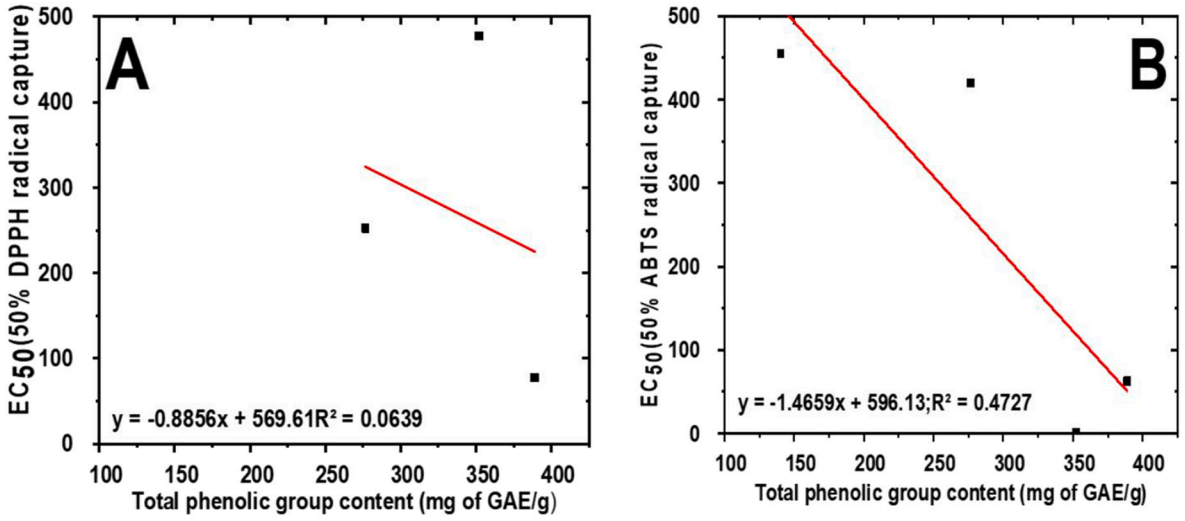

Fig. 9. Correlation between total phenols expressed in milligrams of gallic acid equivalent (mg GAE/g) and antioxidant activity, expressed as 50 % capture concentration of DPPH radicals (A) ABTS (B) (EC_{50} μg/mL).

Table 13
Cytotoxicity results promoted by lignins from branches and leaves of *Protium puncculatum* (PPB and PPL), and *Scleronema micranthum* (SMB and SML) and standard drugs against different cells and mammals (CC_{50} μg/mL) and hemolytic activity (percentage of hemolysis) *in vitro*.

Samples	Macrophage J774 CC_{50} (μg/mL)	Fibroblast (V79) CC_{50} (μg/mL)	Vero Cell CC_{50} (μg/mL)	Hepg2 CC_{50} (μg/mL)	Hemolysis (%)
PPB	34.20 ± 0.1	94.56 ± 0.1	95.0 ± 0.9	>100	< 5.0
PPL	36.51 ± 0.3	96.45 ± 0.1	97.0 ± 0.1	>100	< 5.0
SMB	28.47 ± 0.26	98.23 ± 0.4	99.0 ± 0.2	>100	< 5.0
SML	22.58 ± 0.61	92.85 ± 0.7	96.0 ± 0.3	>100	< 5.0
Amphotericin B	34.75 ± 1.4	76.45 ± 0.1	93.64 ± 0.3	32.9 ± 0.1	~5.0
Benznidazole	32.24 ± 0.1	80.56 ± 0.3	92.1 ± 0.1	>100	~5.0
Praziquantel	28.03 ± 0.9	36.99 ± 0.8	44.99 ± 0.3	>100	<10.0
Chloroquine	>100	>100	> 100	>100	~5.0
Dihydroxyartemizine	> 100	>100	> 100	>100	~5.0

Mean ± Standard Deviation.

The results (Fig. 10A) showed that in a period of 24 h the parasites were in the log phase of growth. In 32 h, the exponential growth phase begins, this period lasted up to 64 h. After this period, the stationary phase begins (72 h of growth) and after 96 h of cultivation, the parasites are in a decline or death phase. Similar results were obtained by Silva et al. [12] evaluating the growth of promastigote forms of *Leishmania amazonensis* in Schneider culture medium, the authors obtained a stationary phase in 72 h.

Fig. 10B shows the exponential growth phase, from which it was possible to determine the growth rate (0.10 h^{-1}), how fast these parasites grow in the culture medium and the generation time (6.93 h), the time required for them to occur. One generation, *i.e.* for the formation of 2 cells from one (binary fission). These vestments may vary according to the growing conditions [12].

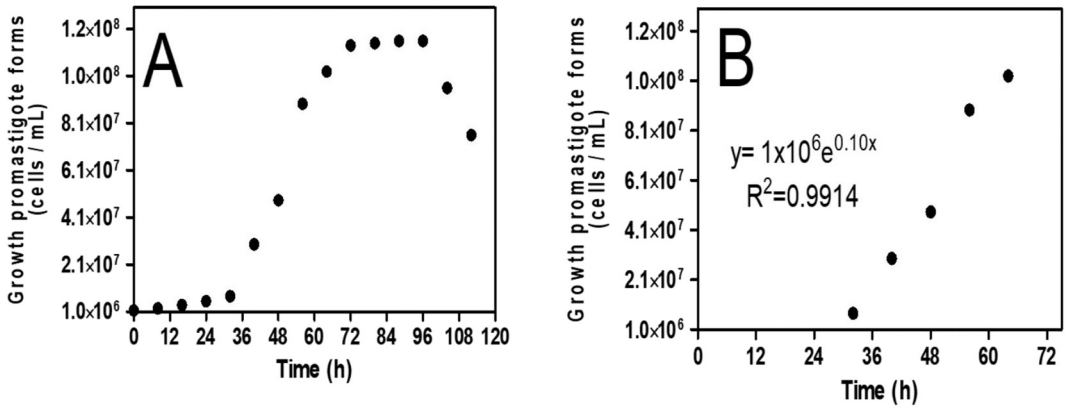

Fig. 10. Growth curve of promastigote forms in Schneider culture medium (A). Representation of the exponential growth phase (B).

The realization of the kinetic growth curve is important because these parasites need to be in the metacyclic promastigote form, the infective form for macrophages. From this parameter (growth time) it is possible to perform cytotoxicity assays in promastigote forms [12]. Fig. 11 shows the results of cytotoxicity promoted by lignins against promastigotes at different concentrations.

Fig. 11 shows that with increasing concentration, there was a significant increase (inhibition of parasite growth ($p < 0.05$). Table 14 presents the IC_{50} results (concentration that inhibits 50 % of promastigote growth) and the selectivity index, that is, how selective the lignin is for the parasite in relation to the macrophage cells.

Table 14 shows that lignins had a lower selectivity index than Amphotericin B (practically 200 times lower). It was also observed that the lignin from the leaves of *Protium puncculatum* showed the highest selectivity against the promastigotes forms, in addition, it showed less cytotoxicity than Amphotericin B. This difference in the selectivity index may be related to the mechanism of action of amphotericin B, when compared to lignins [12].

The mechanism of action of amphotericin B against parasites of the genus Leishmania is related to the binding of this drug to ergosterol/episterol, the main sterols present in the cell membrane of these parasites [12]. The existence of this connection favors the production of micelles, which in turn favor the formation of transmembrane channels that alter the permeability of the membrane, causing an osmotic imbalance, promoting loss of ions and cellular constituents. In mammalian cells, amphotericin B binds to cholesterol forming a low-affinity bond that can generate several side effects. These findings show the efficiency of amphotericin B against these parasites [12].

Table 14
Results of the cytotoxic effect promoted by lignins in a study on the promastigote forms of *Leishmania amazonensis.*

Lignins	IC_{50} (μg/mL)	SI (CC_{50}/IC_{50})
Protium puncticulatum branches	24.9 ± 0.1	1.4
Protium puncticulatum leaves	22.3 ± 0.2	1.6
Scleronema micranthum branches	26.31 ± 0.0	1.1
Scleronema micranthum leaves	20.32 ± 0.1	1.3
Amphotericin B	0.14 ± 0.0	248

Mean ± Standard Deviation.

As lignins have a complex chemical structure and are larger in size when compared to amphotericin B, they do not have a well-established mechanism. However, it is known that they can promote different types of damage to the surface of the parasite and when they cross the cell membrane, they can promote damage to the organelles [12]. Therefore, the prerequisite to evaluate the potential of lignins against different parasites is to verify if they are less toxic to the parasite when compared to animal cells. The lignins evaluated in our study are promising antiparasitic agents, as they are more toxic to the promastigote form of *Leishmania amazonensis* when compared to macrophage cells J774.A1. These results corroborate those obtained by Silva et al. [12] evaluating the antipromastigote effect of an alkaline lignin from *Morinda citrifolia.*

In addition to cytotoxicity assays using the MTT method, ultrastructural analysis was performed using scanning electron microscopy and transmission electron microscopy. These tests were carried out to

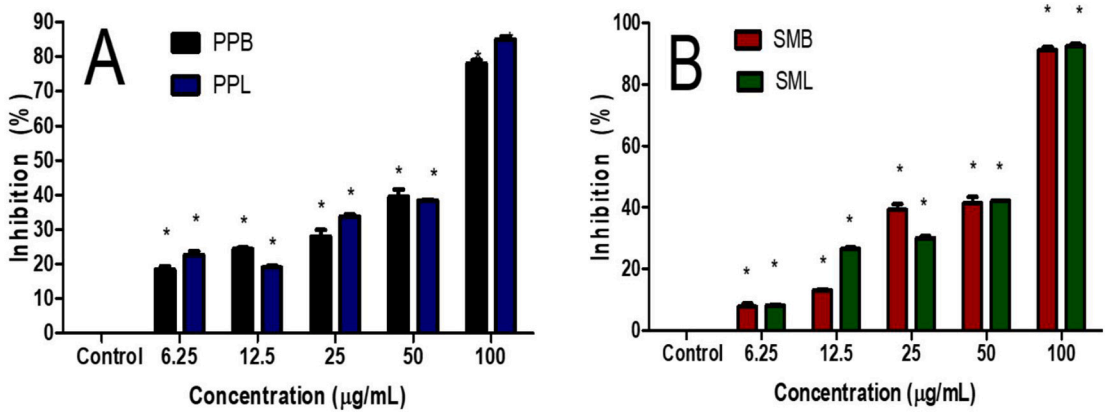

Fig. 11. Cytotoxicity results against *Leishmania amazonensis* promastigote cells. Cytotoxicity promoted by lignins obtained from the branches and leaves of *Protium puncticulatum* (PPB and PPL) (A). Cytotoxicity promoted by lignins obtained from branches and leaves of *Scleronema micranthum* (SMB and SML) (B) at different concentrations (6.25–100 μg/mL) respectively. These results were expressed as mean ± standard deviation. Statistical evaluation was performed using analysis of variance (ANOVA) for multiple comparisons, followed by Tukey's post-test. p values <0.05 were considered significant.

observe the effects produced by the lignins on the parasite surface and at the level of the organelles.

Fig. 12 shows the results of ultrastructural analysis by scanning electron microscopy (SEM) for the lignins obtained from the branches and leaves of *Protium puncticulatum* and *Scleronema micranthum* respectively.

Ultrastructural analyzes by scanning electron microscopy of cells treated with IC_{50} of lignins showed significant morphological changes in the parasites. Among the alterations observed, we highlight the loss of the elongated shape of the cells and drastic alterations observed in the cell membrane of the parasites in relation to the untreated control. The alterations resembled those caused by Amphotericin B.

Only one study was found using lignins with antipromastigote activity, which was carried out by Silva et al. [12] evaluating the antipromastigote effect of an alkaline lignin from *Morinda citrifolia*. However, he knows that different phenolics can promote these alterations, among which we can mention the work developed by Neto et al. [27] who isolated a yangambin lignan obtained from *Ocotea duckei*Vattimo (Lauraceae), which showed antileishmania activity against promastigote forms of *Leishmania chagasi* and *Leishmania amazonensis* observed the same alterations found in our study.

In addition to scanning electron microscopy (SEM) analysis, transmission electron microscopy (TEM) analyzes were performed. MET analyzes were performed in order to evaluate the effect promoted on the parasites' organelles.

Fig. 13 shows the results of ultrastructural analysis by transmission electron microscopy (TEM) for the lignins obtained from the branches and leaves of *Protium puncticulatum*, and *Scleronema micranthum* respectively.

Fig. 13 A shows the photomicrograph of the negative control promastigote form (cells and culture medium) for a 72-h growth period. The parasites showed elongated morphology and homogeneous cytoplasm, in addition to the preservation of organelles. These characteristics in relation to morphology confirm the results obtained by SEM. Fig. 13B presents results referring to the parasites treated with amphotericin B, it can be observed a change in morphology, destruction of organelles and plasma membrane. These results were obtained for lignins from branches and leaves of *Protium puncticulatum* (Fig. 13C and D) and *Scleronema micranthum* (Fig. 13E and F). These results confirm the efficiency of the lignins evaluated in this work against promastigote forms of *Leishmania amazonensis.*

3.6. Trypanocidal activity against the trypomastigote form

The results of cytotoxicity promoted by lignins compared to the standard drug benznidazole against the trypomastigote form are presented in Table 15. Due to the fact that parasites of the genus *Leishmania* also have an affinity for macrophages, the results of the selectivity index for trypomastigotes were also calculated.

The results presented in Table 15 show that the lignins of *Scleronema micranthum* were more cytotoxic against the trypomastigotes forms of *Trypanosoma cruzi* when compared to the lignins of *Protium puncculatum*. However, when it comes to selectivity, *Protium punciculatum* lignins showed a higher selectivity index. In addition, the selectivity indexes obtained for the two lignins were lower when compared to the standard drug presented.

This difference in selectivity may be associated with the mechanism of action. The drug activity takes place through intermediate nucleophilic metabolites [28]. The nitro group (NO_2) present in the Benznidazole molecule is reduced to the amino group (NH_2) through the action of nitroreductor-type enzymes that act specifically in RNO_2 molecular systems [29]. The nitro radical formed in this process would be acting on the trypanocidal effect of Benznidazole through covalent bonds with macromolecules of the parasite: nuclear and mitochondrial DNA, lipids and proteins have recently reinforced this idea, showing that at the molecular level there is a break in the double strand of DNA and damage to the Mitochondrial DNA in tests performed on genetically modified cells exposed to Benznidazole [28].

Another mechanism of action of Benznidazole would be through the increase of phagocytosis acting in the elevation of the production of the cytokine interferon gamma (INF-γ), causing cell lysis [28,29]. On the other hand, the mechanism of action of lignins has not yet been

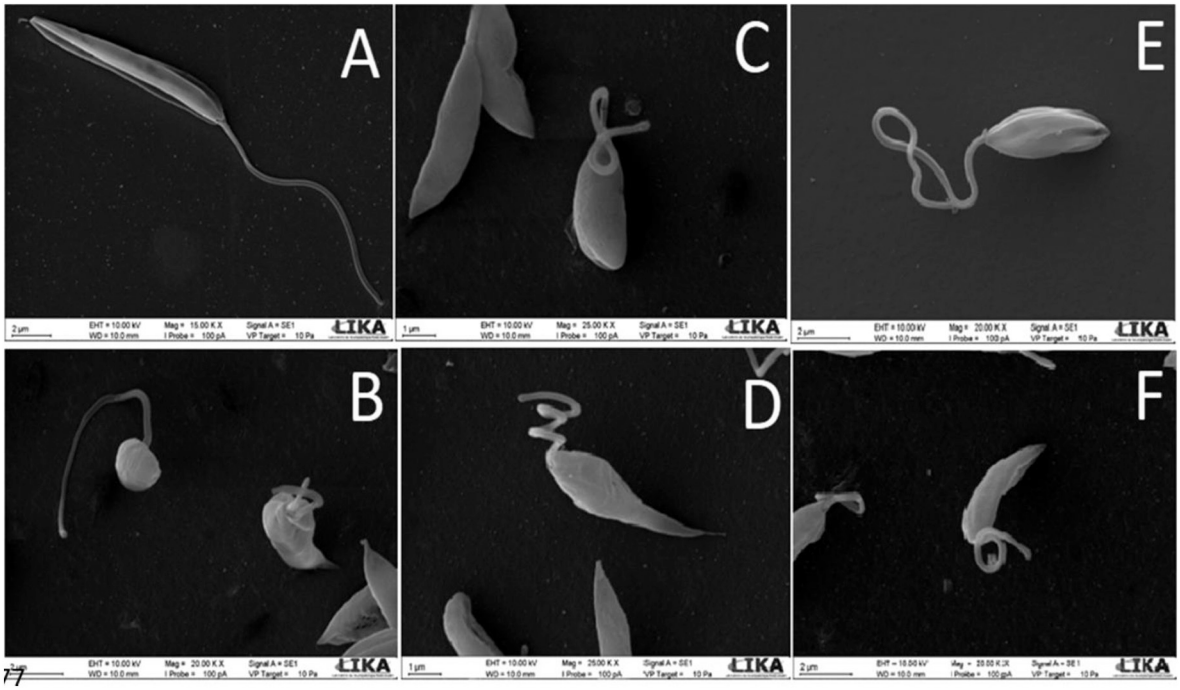

Fig. 12. Electromicrographs of untreated and lignin-treated L. *amazonensis*. Untreated promastigotes with fusiform shape, normal organelle structure (A). Amphotericin B-treated promastigotes (B). Lignins from branches (C) and leaves (D) of *Protium puncticulatum*. Lignins from branches (E) and leaves (F) of *Scleronema micranthum* respectively.

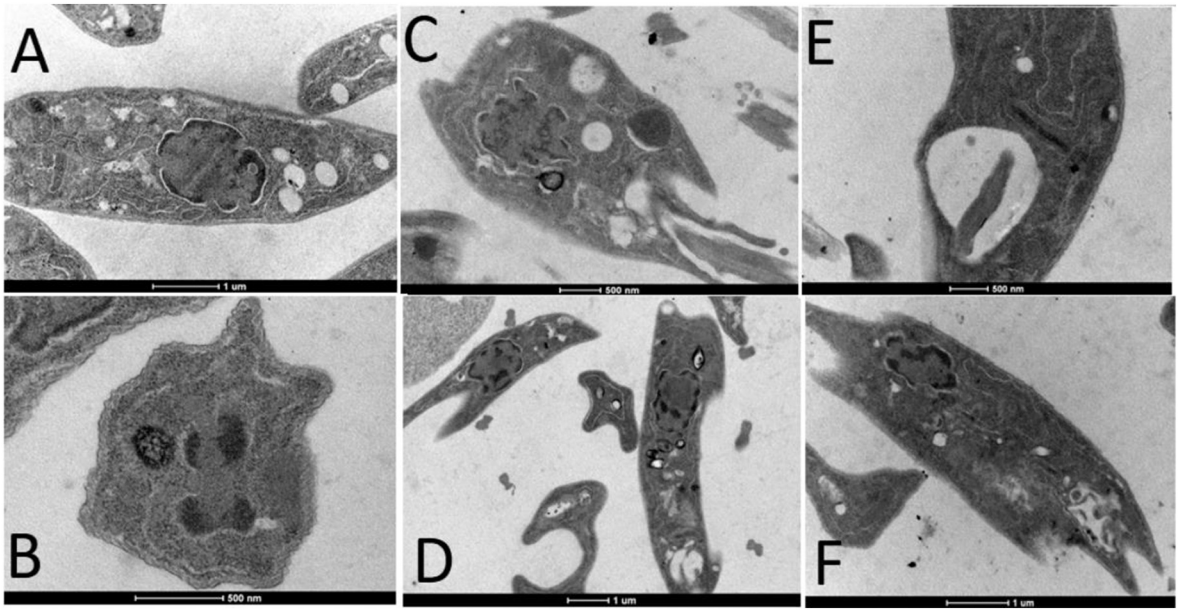

Fig. 13. Electromicrographs of untreated and lignin-treated *L. amazonensis*. Untreated promastigotes with fusiform shape, normal organelle structure (A). Amphotericin B-treated promastigotes (B). Lignins from branches (C) and leaves (D) of *Protium puncticulatum*. Lignins from branches (E) and leaves (F) of *Scleronema micranthum* respectively.

Table 15
Results of the cytotoxic effect promoted by lignins in a study and benznidazole on trypomastigotes forms of *Trypanosoma cruzi*.

Samples	IC_{50} (μg/mL)	SI (CC_{50}/IC_{50})
Protium puncticulatum branches	20.34 ± 0.5	1.7
Protium puncticulatum leaves	19.41 ± 0.1	1.9
Scleronema micranthum branches	17.89 ± 0.3	1.6
Scleronema micranthum leaves	15.54 ± 0.2	1.45
Benznidazole	1.1 ± 0.0	29

Mean ± Standard Deviation.

elucidated, however it is known that these macromolecules can promote antiparasitic effects on the surface of cells due to the different functional groups, mainly the phenolic groups, present in their chemical structure [29].

To date, no studies have been reported evaluating the cytotoxicity of lignins against trypomastigotes. However, some works involving lignans, a group of polyphenols found in different plants, have been reported. Among the works we can mention the works of García-Huertas et al. [30] and Brito et al. [31] evaluating different lignans against the *Trypanosoma cruzi* parasite.

3.7. In vitro schistosomicidal activity

The results of *in vitro* schistosomicidal activity showed that lignins were not able to inhibit *Schistosoma mansoni* growth at different growth stages at different concentrations (25, 50, 100, 200 and 400 μg/mL). This non-activity may be related to the size of the lignins, since other smaller lignioids are capable of promoting the death of these parasites. Silva et al. [32] found that furofuran lignans exhibit schistosomicidal and trypanocidal activities. Parreira et al. [33] evaluating six dibenzylbutyrolacton lignans: hynokinin (1), cubebin (2), yatein (3), 5-methoxylateine (4), dihydrocubebin (5) and dihydroclusin (6) isolated from *Piper cubeba* seed extract were evaluated against *Schistosoma mansoni*. The results showed that all lignans, except 5, were able to separate adult worm pairs and reduce the number of eggs during 24 h of incubation.

3.8. Anti-Plasmodium falciparum activity in vitro

Knowing that erythrocytes are the main cells infected by the parasite *Plasmodium falciparum*, anti-*Plasmodium falciparum* assays were performed using chloroquine-sensitive and resistant strains (internalized in erythrocytes). Thus, molecules with high efficiency against these parasites generally need to have low toxicity against erythrocytes [13]. Fig. 14 shows the results of anti-*Plasmodium falciparum* activity against *Plasmodium falciparum* 3D7 (Fig. 14A) and *Plasmodium falciparum* Dd2 (Fig. 14B) strains. As experimental controls, the drugs chloroquine (for a sensitive strain) and Dihydroartemisinin (for a resistant strain) were used.

The results showed low inhibition values (< 20 %) promoted by lignins against chloroquine-sensitive strains. Regarding the resistant strain, the results were lower than 5 %, indicating that the lignins in this study do not have an inhibitory effect against the resistant strain. These low results may be related to the non-interaction of lignin with the parasite (the parasites are found inside the erythrocytes).

The literature presents few works with *in vitro* anti-*Plasmodium falciparum* activity, promoted by lignins. Recently, Araújo et al. [13] evaluating two lignins obtained from branches and leaves of *Buchenavia viridiflora*, they obtained IC_{50} values of 5592.38 ng/mL (branches lignin) and 2511.44 ng/mL (leaves lignin) for the *Plasmodium falciparum* 3D7 strain. Furthermore, they showed activity against the *Plasmodium falciparum* Dd2 strain with an IC_{50} of 9760 ng/mL (twig lignin) and 2440 ng/mL (leaf lignin) respectively. Other lignoids also promoted anti-*Plasmodium falciparum* activity *in vitro*. Among these we can cite the works carried out by Andrade-Neto et al. [34] and Ortet et al. [35] evaluating different lignins obtained good results against *Plasmodium falciparum* strains. These findings show that lignins may have potential cytotoxic activity against *Plasmodium falciparum* parasites.

3.9. Use of lignins as an excipient for the release of benznidazole, a commercial antiparasitic

Lignins have attracted a lot of attention because they can be used as an excipient to improve the release of drug compounds, because, in addition to being biodegradable and presenting low toxicity, they can promote different biological activities, which can generate a duality of

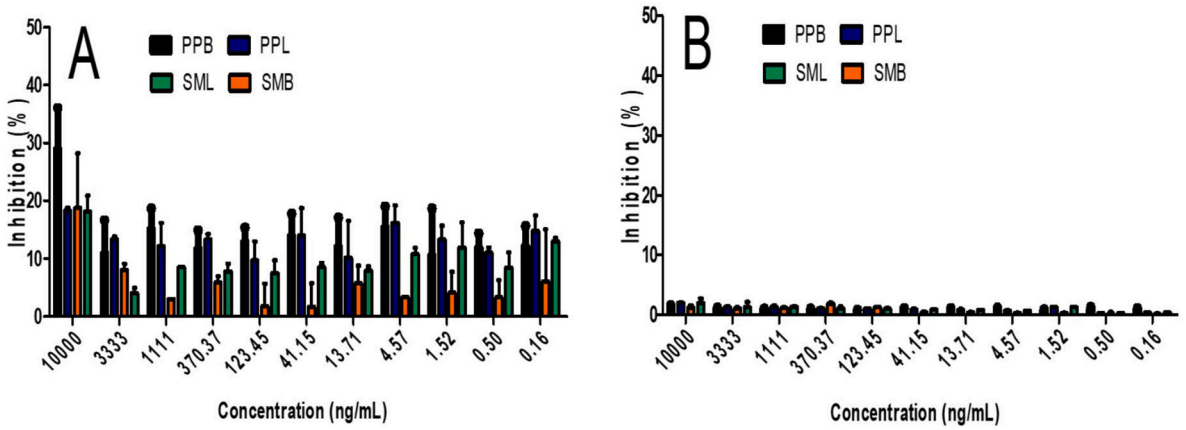

Fig. 14. Results of antiplasmodium activity promoted by lignins obtained from branches and leaves of *Protium puncticulatum* (PPB and PPL) and by branches and leaves of *Scleronema micranthum* (SMB and SML), against the strains *Plasmodium falciparum* 3D7 (A) and *Plasmodium falciparum* Dd2 (B). Results were expressed as mean ± standard deviation.

effects [21].

In addition to these advantages, lignins are available in abundant quantities, as they are generated as a co-product in pulp production processes, which makes them an economically attractive raw material [5,6]. Therefore, tablet formulations containing lignins as an excipient and a control formulation without lignin were carried out. The drug chosen was benznidazole, a trypanocidal drug (in addition, lignins showed more promising IC_{50} values when compared to other antiparasitic activities evaluated in this study) [19].

Initially the formulations were evaluated for disintegration time, the time required for a solid oral dosage form such as a tablet or capsule to completely disintegrate [21]. And a hardness analysis that makes it possible to determine the mechanical strength of the tablets [36]. Finally, dissolution was evaluated in order to evaluate the release kinetics over time. Fig. 15 shows the results of disintegration time (Fig. 15A), hardness (Fig. 15B) and benznidazole dissolution kinetics (Fig. 15C).

The results presented in Fig. 15A showed that the tablet formulations containing lignin promoted an increase in the disintegration time in the following order SMB > PPB > SML > PPL with times varying from 40 to 60 min. In addition, it was observed through Fig. 15B that the lignins with a longer disintegration time had a higher hardness. Following the same order as the disintegration time. The increase in hardness of tablets with lignin may be related to the interaction of this macromolecule with other constituents of the formulation, which may act as a binder, thus increasing tablet hardness Pishnamazi et al. [21]. These results corroborate those obtained by Pishnamazi et al. [36] where it was verified that the hardness of the tablet can influence the disintegration time of the tablet, that is, the greater the hardness, the greater the disintegration time. Thus, it can be observed that the lignins promoted an increase in disintegration time and hardness when compared to the control formulation.

The results presented by Fig. 15C show that the dissolution presented the same tendency of the disintegration time experiments, that is, the benznidazole was released more slowly with the lignins as an excipient in the following order SMB > PPB > SML > PPL. The formulation containing SMB lignin as an excipient is highlighted, indicating a more prolonged release when compared to other lignins and the standard formulation. This release over a longer period of time promotes the maintenance of drug concentration in the bloodstream.

In the literature, several controlled release systems using lignins as an excipient are used. Among these we can mention the works carried out by Pishnamazi et al. [36] evaluating the controlled release of paracetamol containing modified lignin. Pishnamazi et al. [21] Gil-Chávez et al. [37] verified the release of ibuprofen in formulations containing Aquasolv lignin. These findings confirm the potentiality of lignins as excipients in the formulation of pills for studying the controlled release of different drugs.

4. Conclusion

The present work presented four lignins extracted from the branches and leaves of *Protium puncticulatum* and *Scleronema micranthum* plants from the Amazon rainforest. The results of the composition analysis

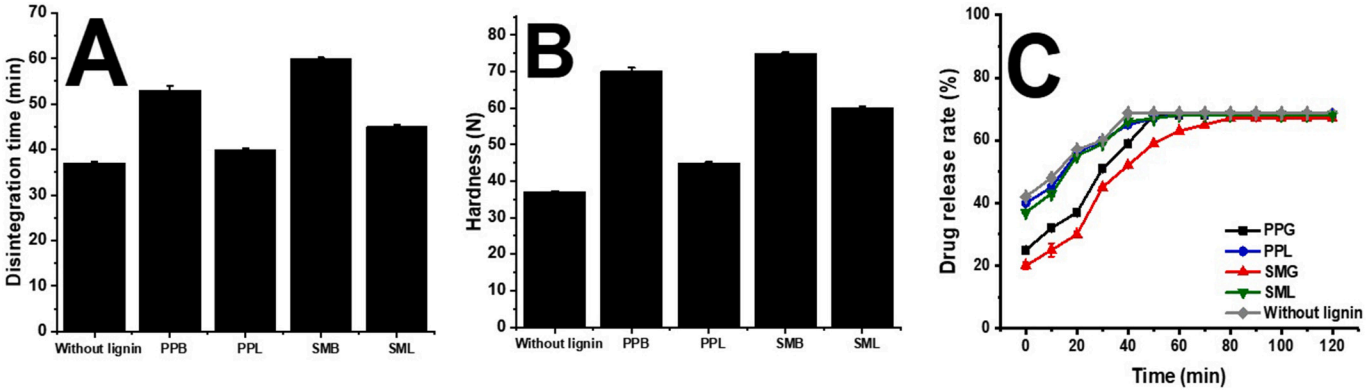

Fig. 15. Results of the disintegration time (A), hardness (B) and drug release rate of benznidazole (C) tests were carried out on tablets without and with lignins obtained from branches and leaves of *Protium puncculatum* (PPB and PPL) and from branches and leaves of *Scleronema micranthum* (SMB and SML).

showed that the contents of the lignocellulosic composition vary according to the region of the plant, that is, branch or leaf. The lignins obtained by acid pretreatment followed by alkaline delignification are of the GSH type, with a predominance of guaiacyl units (G). And they are different from each other, as shown by the results of spectroscopic analysis and the radar tool (used to compare lignins from different sources). The lignins in this study showed promising results of antioxidant activity for the ABTS and DPPH radical scavenging assays and low toxicity against animal cells. *In vitro* antileishmanial activity assays have shown promising results against promastigotes. Moreover, it was able to promote the inhibition of the trypomastigote form of *T. cruzi*. Regarding the anti- *Plasmodium* assays, the lignins showed low activity against *Plasmodium falciparum* strain 3D7 (chloroquine-sensitive) and did not promote toxicity against *Plasmodium falciparum* strain Dd2 (chloroquine-resistant). These low anti-*Plasmodium falciparum* results may be associated with the size of the lignin structure. Lignins do not promote schistosomicidal activity. Finally, we found that lignins are promising excipients in pharmaceutical formulations, helping to release an antiparasitic, benznidazole.

CRediT authorship contribution statement

Iranildo José da Cruz Filho: Conceptualization, Methodology, Formal analysis, Resources, Writing – original draft, Writing – review & editing, Supervision, Project administration. **Denise Maria Figueiredo Araujo Duarte:** Conceptualization, Investigation, Methodology, Validation, Formal analysis, Writing – original draft, Writing – review & editing. **Douglas da Conceição Alves de Lima:** Conceptualization, Investigation, Methodology, Validation, Formal analysis, Writing – original draft, Writing – review & editing. **Diego Santa Clara Marques:** Conceptualization, Investigation, Methodology, Validation, Formal analysis, Writing – original draft, Writing – review & editing. **Fábio André Brayner dos Santos:** Conceptualization, Investigation, Methodology, Validation, Formal analysis, Writing – original draft, Writing – review & editing. **Luiz Carlos Alves:** Conceptualization, Investigation, Methodology, Validation, Formal analysis, Writing – original draft, Writing – review & editing. **André de Lima Aires:** Conceptualization, Investigation, Methodology, Validation, Formal analysis, Writing – original draft, Writing – review & editing. **Fátima Nogueira:** Conceptualization, Investigation, Methodology, Validation, Formal analysis, Writing – original draft, Writing – review & editing. **Maria do Carmo Alves de Lima:** Conceptualization, Methodology, Formal analysis, Resources, Writing – original draft, Writing – review & editing, Supervision, Project administration.

Declaration of competing interest

The authors declare that they have no known competing financial interests or personal relationships that could have appeared to influence the work reported in this paper.

Data availability

Data will be made available on request.

Acknowledgment

This study was funded by the Brazilian agencies Fundação de Amparo à Pesquisa do Estado de Pernambuco - FACEPE (Process APQ-0498-4.03/19), FACEPE (Process APQ-1181-4.03/22) and researcher fixation grant – FACEPE (Process BFP -0038-04.03/21). This study was financed in part by the Coordination for the Improvement of Higher Education Personnel - Brazil (CAPES) - Finance Code 001 and the National Council for Scientific and Technological Development - CNPq (Process 306865/2020-3). We would like to thank Mil Madeiras Preciosas, a subsidiary of the Swiss group Precious Woods (http://preciouswoods.com.br/) for providing samples of branches and leaves of *Protium puncticulatum* and *Scleronema micranthum*. We also thank the Laboratory of Magnetic Resonance of the Institute of Chemistry and Biotechnology (Federal University of Alagoas- UFAL) for the analysis of NMR. Thanks to MR4, who provided us with the *Plasmodium falciparum* MRA-1029 strain provided by Andrew Talman, Robert Sinden that we used in the assays. The work was partially supported by FCT project reference CIRCNA/BRB/0281/2019_AMAZING and GHTM-UID/Multi/04413/2013.

References

[1] A. Beaucamp, M. Muddasar, T. Crawford, M.N. Collins, M. Culebras, Sustainable lignin precursors for tailored porous carbon-based supercapacitor electrodes int, J. Biol. Macromol. 221 (2022) 1142–1149, https://doi.org/10.1016/j.ijbiomac.2022.09.097.

[2] P. Jędrzejczak, M.N. Collins, T. Jesionowski, Ł. Klapiszewski, The role of lignin and lignin-based materials in sustainable construction – a comprehensive review, Int. J. Biol. Macromol. 187 (2021) 624–650, https://doi.org/10.1016/j.ijbiomac.2021.07.125.

[3] P.S. Chauhan, R. Agrawal, A. Satlewal, R. Kumar, R.P. Gupta, S.S.V. Ramakumar, Next generation applications of lignin derived commodity products and their life cycle, techno-economical and societal analysis, Int. J. Biol. Macromol. 197 (2021) 179–200, https://doi.org/10.1016/j.ijbiomac.2021.12.146.

[4] C.C. Xu, L. Dessbesell, Y. Zhang, Z. Yuan, Lignin valorization beyond energy use: has lignin's time finally come? Biofpr 15 (1) (2021) 32–36, https://doi.org/10.1002/bbb.2172.

[5] A. Beaucamp, M. Muddasar, I.S. Amiinu, M.M. Leite, M. Culebras, K. Latha, M. C. Gutiérrez, D. Rodriguez-Padron, F. del Monte, T. Kennedy, Lignin for energy applications–state of the art, life cycle, technoeconomic analysis and future trends, Green Chem. 24 (2022) 8193–8226, https://doi.org/10.1039/D2GC02724K.

[6] M. Stanisz, Ł. Klapiszewski, M.N. Collins, T. Jesionowski, Recent progress in biomedical and biotechnological applications of lignin-based spherical nano- and microstructures: a comprehensive review, Mater. Today Chem. 26 (2022), 101198, https://doi.org/10.1016/j.mtchem.2022.101198.

[7] L. Zheng, G. Lu, W. Pei, W. Yan, Y. Li, L. Zhang, Q. Jiang, Understanding the relationship between the structural properties of lignin and their biological activities, Int. J. Biol. Macromol. 190 (2021) 291–300, https://doi.org/10.1016/j.ijbiomac.2021.08.168.

[8] I.J. Cruz Filho, B.R. da Silva Barros, L.M. de Souza Aguiar, C.D.C. Navarro, J. S. Ruas, V.M.B. de Lorena, A.M.S. Maior, Lignins isolated from prickly pear cladodes of the species opuntia fícus-indica (Linnaeus) miller and Opuntia cochenillifera (Linnaeus) miller induces mice splenocytes activation, proliferation and cytokines production, Int. J. Biol. Macromol. 123 (2019) 1331–1339, https://doi.org/10.1016/j.ijbiomac.2018.09.120.

[9] D.K.D. Santos, B.R. da Silva Barros, L.M. de Souza Aguiar, I.J. da Cruz Filho, V.M. B. de Lorena, C.M.L. de Melo, T.H. Napoleão, Immunostimulatory and antioxidant activities of a lignin isolated from Conocarpus erectus leaves, Int. J. Biol. Macromol. 150 (2020) 169–177, https://doi.org/10.1016/j.ijbiomac.2020.02.052.

[10] M.D.M. Arruda, S.D.P.L. Alves, I.J. da Cruz Filho, G.F. de Sousa, G.A. de Souza Silva, D.K.D. do Nascimento Santos, C.M.L. de Melo, Characterization of a lignin from Crataeva tapia leaves and potential applications in medicinal and cosmetic formulations, Int. J. Biol. Macromol. 180 (2021) 286–298, https://doi.org/10.1016/j.ijbiomac.2021.03.077.

[11] C.M.L. Melo, I.J. da Cruz Filho, G.F. de Sousa, G.A. de Souza Silva, D.K.D. do Nascimento Santos, R.S. da Silva, G.J. de Moraes Rocha, Lignin isolated from Caesalpinia pulcherrima leaves has antioxidant, antifungal and immunostimulatory activities, Int. J. Biol. Macromol. 162 (2020) 1725–1733, https://doi.org/10.1016/j.ijbiomac.2020.08.003.

[12] P.R. Silva, M.D.C.A. de Lima, T.P. Souza, J.M. Sandes, A.D.C.A. de Lima, P.J. R. Neto, I.J. da Cruz Filho, Lignin from Morinda citrifolia leaves: physical and chemical characterization, in vitro evaluation of antioxidant, cytotoxic, antiparasitic and ultrastructural activities, Int. J. Biol. Macromol. 193 (2021) 1799–1812, https://doi.org/10.1016/j.ijbiomac.2021.11.013.

[13] D.M.F. Araújo, I.J. da Cruz Filho, T. Santos, D.T.M. Pereira, D.S.C. Marques, A.D.C. A. de Lima, F. Nogueira, Biological activities and physicochemical characterization of alkaline lignins obtained from branches and leaves of Buchenavia viridiflora with potential pharmaceutical and biomedical applications, Int. J. Biol. Macromol. 219 (2022) 224–245, https://doi.org/10.1016/j.ijbiomac.2022.07.225.

[14] E. Chiani, A. Beaucamp, Y. Hamzeh, M. Azadfallah, A.V. Thanusha, M.N. Collins, Synthesis and characterization of gelatin/lignin hydrogels as quick release drug carriers for ribavirin, Int. J. Biol. Macromol. 224 (2023) 1196–1205, https://doi.org/10.1016/j.ijbiomac.2022.10.205.

[15] M. Culebras, M. Pishnamazi, G.M. Walker, M.N. Collins, Facile tailoring of structures for controlled release of paracetamol from sustainable lignin derived platforms, Molecules 26 (2021) 1593, https://doi.org/10.3390/molecules26061593.

[16] V.C. Silva, C.M. Rodrigues, Natural products: an extraordinary source of value-added compounds from diverse biomasses in Brazil, Chem. biol. technol. 1 (1) (2014) 1–6, https://doi.org/10.1186/s40538-014-0014-0.

[17] M.C.N.D. Andrade, C. Sales-Campos, C.S.M.D. Carvalho, L.V.B.D. Aguiar, M.T.D. A. Minhoni, Uso de resíduos madeireiros da Amazônia Brasileira no cultivo in vitro

de lentinus strigosus use of wood waste from the brazilian Amazon in the in vitro cultivation of lentinus strigosus, Ambiência 9 (1) (2013) 189–196.
[18] A. Albiero-Júnior, A. Venegas-González, P.C. Botosso, F.A. Roig, J.L.C. Camargo, M. Tomazello-Filho, What is the temporal extension of edge effects on tree growth dynamics? A dendrochronological approach model using Scleronema micranthum (Ducke) ducke trees of a fragmented forest in the Central Amazon, Ecol. Indic. 101 (2019) 133–142, https://doi.org/10.1016/j.ecolind.2018.12.040.
[19] L.H. Rosa, V.N. Gonçalves, R.B. Caligiorne, T. Alves, A. Rabello, P.A. Sales, C. L. Zani, Leishmanicidal, trypanocidal, and cytotoxic activities of endophytic fungi associated with bioactive plants in Brazil, Braz. J. Microbiol. 41 (2010) 420–430.
[20] A.S. Pereira, G.O. Silveira, M.S. Amaral, S.M. Almeida, J.F. Oliveira, M.C. Lima, S. Verjovski-Almeida, In vitro activity of aryl-thiazole derivatives against Schistosoma mansoni schistosomula and adult worms, PLoS One 14 (11) (2019), e0225425.
[21] M. Pishnamazi, J. Iqbal, S. Shirazian, G.M. Walker, M.N. Collins, Effect of lignin on the release rate of acetylsalicylic acid tablets, Int. J. Biol. Macromol. 124 (2019) 354–359.
[22] A.L.M.D. Silva, J.L. Soares Sobrinho, P.J. Rolim Neto, R.M.F.D. Silva, F.P.M. D. Medeiros, L.G.D. Lima, Desenvolvimento de método analítico por CLAE em comprimidos de benznidazol Para a Doença de chagas, Quím. Nova 30 (2007) 1163–1166.
[23] R.D.D. Araújo, Evaluation of the Potential of Managed Species in the Amazon for the Production of Non-structural "EGP" Panels, 2019.
[24] C.S. Nascimento, Efeito de extrativos obtidos de Espécies florestais impregnados em Madeira de simaruba Amara (marupá) e submetidos ao ataque de nasutitermes sp, (isoptera. VIII Jornada de Iniciação Cientifica do INPA, 1999.
[25] C.A.E. Costa, P.C.R. Pinto, A.E. Rodrigues, Radar tool for lignin classification on the perspective of its valorization, Ind. Eng. Chem. Res. 54 (31) (2015) 7580–7590, https://doi.org/10.1021/acs.iecr.5b01859.
[26] C.A.E. Costa, W. Coleman, M. Dube, A.E. Rodrigues, P.C.R. Pinto, Assessment of key features of lignin from lignocellulosic crops: stalks and roots of corn, cotton, sugarcane, and tobacco, Ind. Crop. Prod. 92 (2016) 136–148.
[27] R.L.M. Neto, L.M. Sousa, C.S. Dias, J.M. Barbosa Filho, M.R. Oliveira, R. C. Figueiredo, Morphological and physiological changes in leishmania promastigotes induced by yangambin, a lignan obtained from Ocotea duckei, Exp. Parasitol. 127 (1) (2011) 215–221, https://doi.org/10.1016/j.exppara.2010.07.020.
[28] J. Müller Kratz, F. Garcia Bournissen, C.J. Forsyth, S. Sosa-Estani, Clinical and pharmacological profile of benznidazole for treatment of chagas disease, Expert. Rev. Clin. Pharmacol. 11 (10) (2018) 943–957, https://doi.org/10.1080/17512433.2018.1509704.
[29] A.L. Mazzeti, P. Capelari-Oliveira, M.T. Bahia, V.C.F. Mosqueira, Review on experimental treatment strategies against trypanosoma cruzi, J. Exp. Pharmacol. 13 (2021) 409, https://doi.org/10.2147/JEP.S267378.
[30] Paola García-huertas, et al., Activity in vitro and in vivo against trypanosoma cruzi of a furofuran lignan isolated from piper jericoense, Exp. Parasitol. 189 (2018) 34–42, https://doi.org/10.1016/j.exppara.2018.04.009.
[31] Juliana R. Brito, et al., Dibenzylbutane neolignans from Saururus cernuus L. (Saururaceae) displayed anti-trypanosoma cruzi activity via alterations in the mitochondrial membrane potential, Fitoterapia 137 (2019), 104251, https://doi.org/10.1016/j.fitote.2019.104251.
[32] M.L.A. Silva, V.R. Esperandim, D. da Silva Ferreira, L.G. Magalhães, T.C. Lima, W. R. Cunha, J.K. Bastos, Furofuran lignans display schistosomicidal and trypanocidal activities, Phytochemistry 107 (2014) 119–125, https://doi.org/10.1016/j.phytochem.2014.08.010.
[33] R.L. Parreira, E.S. Costa, V.C. Heleno, L.G. Magalhães, J.M. Souza, P.M. Pauletti, M. L. Andrade e Silva, Evaluation of lignans from Piper cubeba against Schistosoma mansoni adult worms: a combined experimental and theoretical study, Chemistry & Biodiversity 16 (1) (2019), e1800305, https://doi.org/10.1002/cbdv.201800305.
[34] V.F. Andrade-Neto, T. da Silva, L.M.X. Lopes, V.E. do Rosário, F. de Pilla Varotti, A. U. Krettli, Antiplasmodial activity of aryltetralone lignans from Holostylis reniformis, Antimicrob. Agents Chemother. 51 (7) (2007) 2346–2350, https://doi.org/10.1128/AAC.01344-06.
[35] R. Ortet, S. Prado, E.L. Regalado, F.A. Valeriote, J. Media, J. Mendiola, O. P. Thomas, Furfuran lignans and a flavone from Artemisia gorgonum Webb and their in vitro activity against plasmodium falciparum, J. Ethnopharmacol. 138 (2) (2011) 637–640, https://doi.org/10.1016/j.jep.2011.09.039.
[36] PIshnamazi, Mahboubeh, Design of controlled release system for paracetamol based on modified lignin, Polymers 11 (6) (2019) 1059, https://doi.org/10.3390/polym11061059.
[37] J. Gil-Chávez, S.S.P. Padhi, C.S. Leopold, I. Smirnova, Application of aquasolv lignin in ibuprofen-loaded pharmaceutical formulations obtained via direct compression and wet granulation, Int. J. Biol. Macromol. 174 (2021) 229–239, https://doi.org/10.1016/j.ijbiomac.2021.01.064.